

**INSTITUTO TECNOLOGICO Y DE ESTUDIOS
SUPERIORES DE MONTERREY
CAMPUS MONTERREY
PROGRAMA DE GRADUADOS DE LA
DIVISION DE ELECTRONICA, COMPUTACION,
INFORMACION Y COMUNICACIONES**



A Joint Source Channel Coding Approach to Delivery of Digital Images
over CDMA 800 MHz Indoor Wireless Rayleigh Fading Channels

Thesis

Presented as a partial fulfillment of the requirements
for the degree of
Master of Science in Electrican Engineering
Major in Telecommunications

Jacobo Murillo Zolezzi

July 2004

**INSTITUTO TECNOLOGICO Y DE ESTUDIOS
SUPERIORES DE MONTERREY
CAMPUS MONTERREY**

Division de Electronica, Computacion, Informacion
y Comunicaciones

PROGRAMA DE GRADUADOS DE LA
DIVISION DE ELECTRONICA, COMPUTACION,
INFORMACION Y COMUNICACIONES

The members of the thesis committee recommended the acceptance of the thesis of
Jacobo Murillo Zolezzi as a partial fulfillment of the requirements for the degree of
Master of Science in

**Electrical Engineering
Major Telecommunications
Thesis Committee**

Dr. Jose Ramon Rodriguez Cruz
Advisor

Dr. Carlos M. Hinojosa Espinosa
Synodal

Dr. Cesar Vargas Rosales
Synodal

Approved

Dr. David Garza Salazar
Director de los Programas de Posgrado
en Electronica, Computacion,
Informacion y Comunicaciones
July 2004

**Instituto Tecnológico y de Estudios
Superiores de Monterrey
Campus Monterrey**
Division de Electronica, Computacion, Informacion y
Comunicaciones
Programas de Graduados en Electronica, Computacion,
Informacion y Comunicaciones

**A Joint Source Channel Coding Approach to Delivery
of Digital Images over CDMA 800 MHz Indoor Wireless
Rayleigh Fading Channels**

Thesis

Presented as a partial fulfillment of the requirements for the degree of
Master of Science in Electrical Engineering
Major Telecommunications

Jacobo Murillo Zolezzi
July 2004

Dedication:

I wish to dedicate this thesis to my parents, who have supported me and given me the opportunities that have allowed me to complete my studies. And whose support and love throughout my studies has been one of the most important factors that has allowed me to grow and prepare myself for this new transition which will mark the start of the rest of my life.

To Sabine who has given me her unconditional love throughout the term of my studies in Mexico and who is soon to become a part of my life forever.

And to my advisor and teachers at the Technological Institute of Monterrey who have imparted on me part of their wisdom and knowledge in the area of telecommunications. Thank you.

Abstract

The following thesis developed in the area of Electrical Engineering and Telecommunications is aimed at improving current CDMA wireless network capabilities specifically targeting the transmission of JPEG compressed data with the possibility of a continued investigation in the transmission of MPEG video format. The aim or objective is to generate a solution to current transmission problems faced in 3rd generation CDMA networks where band limited transmission limits the capabilities of the network in delivering large data files such as image or video adequately.

The rising importance in expanding network capabilities for CDMA networks, in this case for image transmission, is evident because of several factors including the following:

- One of these factors is the increasing popularity of CDMA since its creation in 1995. In the cellular branch alone, there are over an estimates 106 million users utilizing a CDMA based network. This rapid increase is due to the fact that CDMA is able to support multiple users on one frequency channel, as will be discussed later.
- Secondly and more importantly, the growing demand for image and video transmission generated by increasing multimedia usage has created the recent need to transmit video data over this and other types of wireless networks.

In particular, the following thesis is thus aimed at improving the JPEG image compression algorithm for an 800MHz CDMA Cellular wireless network. In order to increase the efficiency of current image transmission over CDMA networks this thesis proposes jointly designing the source and channel code to generate an enhanced image compression algorithm. In order to accomplish this we will utilize a Rayleigh Fading Model to simulate the channel over which we will be transmitting and then include this information into the compression algorithm; our goal being to manipulate the image compression algorithm to improve image transmission over a specific channel and medium (i.e. An 800MHz wireless network).

Furthermore, given that our expected results are met, we can also review the efficiency (bit compression) of our algorithm for transmission and hence review new possibilities for increased error correction in the transmission of image and video data. In addition, as mentioned before, an ongoing investigation in this area using the ideas presented in this paper applied to the MPEG compression algorithm could lead to an enhanced algorithm for video transmission over the same medium.

Contents

1	Introduction	2
1.1	Motivation	3
1.2	Justification & Objective	4
1.3	Contribution	4
2	Background, Concepts & Terminology	5
2.1	Joint Source Channel Coding	5
2.2	Graphical Overview	5
2.3	Mathematical Overview of Proposed Model	6
2.4	Source Coding	8
2.4.1	JPEG	8
2.4.2	Baseline JPEG	10
2.4.3	Sub-Sampling (For Color Images)	10
2.4.4	Discrete Cosine Transform	11
2.4.5	Quantization	13
2.4.6	Entropy Coding	16
2.5	A Brief Review and Comparison Between JPEG and MPEG Coding	17
2.5.1	What is MPEG?	17
2.5.2	JPEG vs MPEG compression algorithms	17
2.6	Channel Coding	18
2.7	Access Technique: CDMA	19
2.7.1	What is Spread Spectrum Communication?	20
2.8	Frequency Modulation	23
2.8.1	QPSK Modulation	23
2.9	Filtering	24
2.10	Channel Type	24
2.10.1	Important Radio Channel Characteristics	26
2.10.2	Characteristics of the Indoor Wireless Channel	27
2.10.3	Indoor Propagation Models	28
2.10.4	Multipath Fading Radio Channel Model: Rayleigh Fading Model	30
2.10.5	BER Approximations for DS-CDMA Communications Systems over Rayleigh Fading Channels	33
3	Joint Source Channel Code Design	35
4	Simulation Overview	36
4.1	.tif to .jpg	37
4.2	Quantization	38

4.2.1	Variable Uniform Quantization	38
4.2.2	Channel Optimized Vector Quantization	38
4.3	Decimal to Binary	41
4.4	Transmission of data	41
4.4.1	The QPSK modulation	41
4.4.2	The CDMA access technique	42
4.4.3	The transmission of the encoded image through a wireless Rayleigh fading channel	44
4.5	Receiver	45
4.6	Binary to decimal	46
4.7	De-Quantization of received coefficients	46
4.8	JPEG decoding	46
5	Results	47
5.1	Original Images	47
5.2	Original Quantized Images	48
5.3	Received Pictures	50
5.4	Generalized Results	56
6	Conclusions	58
6.1	Future Work	59
A	Additional Results	60

List of Tables

2.1	Sampling of Color Images	11
2.2	Multipath Channel Characteristics, Models, and Operational Environments .	27
2.3	Average Signal Loss Measurements for Radio Paths Obstructed by Common Building Materials	29
2.4	Average Signal Loss Measurements for Radio Paths Obstructed by Floor Separations	30
2.5	Average Signal Loss Measurements for Radio Paths Obstructed by Common Building Materials	30
2.6	Mean and Variance for Different Modulation Schemes	34
5.1	Results for tire.tif and cameraman.tif	57

List of Figures

2.1	Graphical Overview of Simulation	6
2.2	JPEG Compression	10
2.3	Available Channel Coding Techniques	20
2.4	DS-CDMA Spreading Technique	21
2.5	DS-CDMA Spreading of Signal	21
2.6	Rayleigh Fading Channel Model $r(t) = \alpha x_m(t) + n(t)$	31
4.1	Vector Quantization	39
4.2	Channel Optimized Vector Quantization	39
4.3	M-Sequence Construction	42
4.4	Frequency Response Nyquist Filter	43
5.1	Original Complete Picture Used in Transmission	47
5.2	Original Fraction of Picture	47
5.3	LVQ Quantization Without Transmission of tire.tif	48
5.4	Lloyds Quantization Without Transmission of tire.tif	48
5.5	LVQ Quantization Without Transmission of Cameraman.tif	49
5.6	Lloyds Quantization Without Transmission of Cameraman.tif	49
5.7	$E_B/N_0=1$ dB Using LVQ Quantization	50
5.8	$E_B/N_0=1$ dB Using Lloyds Quantization	50
5.9	$E_B/N_0=2$ dB Using LVQ Quantization	51
5.10	$E_B/N_0=2$ dB Using Lloyds Quantization	51
5.11	$E_B/N_0=3$ dB Using LVQ Quantization	52
5.12	$E_B/N_0=3$ dB Using Lloyds Quantization	52
5.13	$E_B/N_0=4$ dB Using LVQ Quantization	53
5.14	$E_B/N_0=4$ dB Using Lloyds Quantization	53
5.15	$E_B/N_0=5$ dB Using LVQ Quantization	54
5.16	$E_B/N_0=5$ dB Using Lloyds Quantization	54
5.17	$E_B/N_0=6$ dB Using LVQ Quantization	55
5.18	$E_B/N_0=6$ dB Using Lloyds Quantization	55
5.19	Resulting MSE using Lloyds vs. LVQ Quantization of tire.tif	56
5.20	Resulting MSE using Lloyds vs. LVQ Quantization of cameraman.tif	57
A.1	$E_B/N_0=1$ dB Using LVQ Quantization	60
A.2	$E_B/N_0=1$ dB Using Lloyds Quantization	60
A.3	$E_B/N_0=2$ dB Using LVQ Quantization	61
A.4	$E_B/N_0=2$ dB Using Lloyds Quantization	61
A.5	$E_B/N_0=3$ dB Using LVQ Quantization	62
A.6	$E_B/N_0=3$ dB Using Lloyds Quantization	62
A.7	$E_B/N_0=4$ dB Using LVQ Quantization	63

A.8	$E_B/N_0=4$ dB Using Lloyds Quantization	63
A.9	$E_B/N_0=5$ dB Using LVQ Quantization	64
A.10	$E_B/N_0=5$ dB Using Lloyds Quantization	64
A.11	$E_B/N_0=6$ dB Using LVQ Quantization	65
A.12	$E_B/N_0=6$ dB Using Lloyds Quantization	65
A.13	$E_B/N_0=10$ dB Using LVQ Quantization	66
A.14	$E_B/N_0=10$ dB Using Lloyds Quantization	66

1 Introduction

The main subject treated in this thesis is a Joint Source Channel Coding (JSCC) quantization optimization to enhance performance over a Rayleigh fading channel. Because the optimization of information transfer over noise channels is an area of great interest and importance, a great deal of research and investigation has been carried out in this area.

One of the papers that dictates the origins of this line of investigation was written by H. Kumazawa, M. Kasahara, and T. Namekawa in 1984, “A construction of Vector Quantizers for noisy channels” [15]. In this paper the authors searched and formulated a criteria for optimality on vector quantizers. The concept became a cornerstone for the development of a series of theories and concepts that lead to applications of Channel Optimized Vector Quantization (COVQ) among other novel techniques.

Other important papers in this area, that are worth mentioning, are written by N. Farvardin. Among them the following two papers, “A study of Vector Quantization for Noisy Channels” [8], and “On the Performance and Complexity of Channel Optimized Vector Quantizers” [9], are of great importance. The first of these papers concentrates on the index assignment issue, and the latter, investigates the design and structure of COVQ’s which is the theme of this thesis.

Besides COVQ, further investigation along similar lines lead to the development of algorithms for soft decoding of VQ over noisy channels. Once again work related to this line of study can be found in Farvardin’s “Joint Design of Block Source Codecs and Modulation Signal Sets” [10], which considers a linear approximation to the generally nonlinear minimum mean-square error (MMSE) decoder for the additive white Gaussian noise (AWGN) channel.

The results of this paper have been thoroughly examined and extended. One important extension, written by F.H. Liu, P.Ho and V. Cuperman leads to the nonlinear optimal decoder explained in the paper “Joint Source and Channel Coding Using a Non-Linear Receiver” [12].

Another important topic, which has been developed recently in this same area of study, is Hadamard-based soft decoding. Although it has been studied in several different works, it was finally generalized to the optimal nonlinear case by M. Skoglund in “A soft decoder Vector Quantizer for A Rayleigh Fading Channel” [28]. This last article, which gives us a brief insight into COVQ, studies several different quantization schemes, among which we find the Hadamard formulation of the optimal decoder, the robust VQ approach, and the channel optimized VQ approach. His study in this area is based on the transmission of information over a Rayleigh fading channel with the following characteristics

$$R_n = A_n \times b_n + W_n \tag{1.1}$$

where R_n is the output of the matched filter at the receiver, W_n is the additive white Gaussian noise, A_n is the white amplitude process and b_n is the binary information.

Furthermore, Skoglund relies on the Hadamard transform which he uses as the key to the implementation of the MMSE decoder. By doing so the Optimal Soft Hadamard Column Decoder (SHCD-OPT) which is developed in his paper, and can be viewed as a SHCD, accounts for a priori information and can be utilized to counteract channel errors. As one of his encoder designs, Skoglund utilizes a channel optimized VQ where the encoder-decoder pair are jointly trained for a specific channel. However, training in his paper is carried out for the SHCD-OPT decoder and is optimized for the expected value of the bit error probability.

In his applications and results we find that the frequency domain of a JPEG image is divided into three different regions: a low, a medium and high frequency region, which are then coded with different VQ's with the highest rate for low frequencies. This thesis proposes using a Discrete Cosine Transform to carry out the source coding, in which a mask of 64 coefficients is used to retain the low frequency coefficients and eliminate the high frequency coefficients. Furthermore, unlike Skoglund, a channel optimized VQ which is jointly trained with a decoder will be developed based on hard decision making hence possibly decreasing the overall complexity of the decoder.

In general, this thesis proposes a jointly designed source and channel code using a channel optimized VQ algorithm with a hard decision based decoder to transmit JPEG DCT compressed images through a Rayleigh fading channel.

1.1 Motivation

During the past few years there has been an increasing interest to expand multimedia communication capabilities, specifically those regarding the transfer of digital images over CDMA based networks. Code division multiple access, otherwise known as CDMA, is a third generation modulation technique with improved capabilities in comparison to the existing time and frequency division multiple access networks (TDMA & FDMA respectively). Its obvious potential has made it one of the leading access techniques for several applications including wireless routers and cellular networks among others, hence its exponential growth ever since its introduction into the market in 1995.

One aspect of specific importance when talking about CDMA networks, in contrast to its other multiple access counterparts, is the use of orthogonal waveforms which allows users to share a given frequency simultaneously in a specified time window. This allows wireless companies to increase the number of users on their allocated wireless spectrum. Because of its potential, CDMA has rapidly grown to become the network standard for wireless communications. However, although it has multiple user capabilities, CDMA still encounters what we may refer to as 'traditional' transmission problems especially when regarding large image or video file transmission.

1.2 Justification & Objective

In order to decrease the effects of a Rayleigh fading channel on the transmission of a large file such as an image, where entropy coding is preferably avoided because of the propagation of errors through the transmitted data, one should consider adopting a JSCC. A JSCC solution aims at increasing the robustness of transmitted information over a specific channel without resorting to parity bits or redundancy that increase the transmission bandwidth in a medium that is limited in size. To achieve a JSCC solution for image transmission over Rayleigh fading channels we choose to employ and simulate a COVQ algorithm where the codebook vectors are trained with additional information from the specific channel in the recursive training algorithm. The COVQ adjusts for established channel noise obtained by modeling the wireless channel using a computerized mathematical model.

In general, the objective of this thesis is to use a JSCC approach in order to optimize a VQ algorithm for specific channel noise using a Matlab programmed mathematical model of a Rayleigh fading channel. Then, by simulating the effects of a wireless indoor channel on image transmission, we will evaluate the performance of our COVQ algorithm and compare our results to present image delivery techniques.

1.3 Contribution

The importance of implementing an enhanced image delivery technique in the multimedia communicated world of today is quite obvious. Every day, as technology advances and computer capabilities increase, the future of personal communications all point toward one goal, a world in which image and video transmission become standard. Hence in the present we are already observing mobile communication devices with the distinct need to obtain acceptable image and video transmission over the same standard networks.

The proposed algorithm aims at increasing the robustness of large image transfer over Rayleigh fading channels while at the same time decreasing the size of the data by avoiding channel coding. The results obtained from this simulation and thesis should demonstrate that by using a JSCC approach and implementing a COVQ scheme that is trained with specific channel noise, we are not only able to decrease the bandwidth of the transmitted data but also make it more robust for the specific channel being considered.

In general, like other authors such as Skoglund, we wish to develop an enhanced algorithm for image transmission over Rayleigh fading channels with specific characteristics. Hence, our contribution in the area of image transmission, is to develop a JSCC technique focused on constructing a COVQ algorithm that targets specific Rayleigh fading channel multipath, noise, and attenuation characteristics. By utilizing channel information in the construction of our COVQ we hope to create a more efficient and reliable transmission algorithm.

2 Background, Concepts & Terminology

In the following section we will review the basic concepts on which this thesis is based on. The information will be reviewed here in a general manner and will later be explained in more detail in the simulation overview, section [4]. In general, this section includes the background information necessary to comprehend the transmission of digital image data using a CDMA multiple access technique, over a Rayleigh fading channel.

2.1 Joint Source Channel Coding

What is Joint Source Channel Coding? A joint source channel coding approach is one that tries to jointly design the source and channel codes to optimize end to end quality for a given transmitted message. We want to use this type of approach on CDMA network based delivery of JPEG data to help us provide reliable delivery of video in the presence of expected channel noise. Specifically, by developing source code utilizing channel information about wireless networks we can manipulate present JPEG compression algorithms to improve the transfer capabilities of wireless networks, thus ultimately improving the quality of end to end image transmission in this type of channel.

2.2 Graphical Overview

As briefly reviewed in the introduction the goal of this thesis is to develop a joint source channel coding design in order to efficiently transfer JPEG coded images over a wireless 800 MHZ channel. In order to achieve this optimization, it is hypothesized that by utilizing an alternate form of compression we will be able to enhance the robustness of our image when transmitted over this specific channel. Specifically, in this thesis we propose changing the standard variable uniform quantization used in JPEG with a channel optimized vector quantization scheme.

Before starting to review the concepts behind the transmission of images over a Rayleigh fading channel we wish to present the following diagram which graphically illustrates the similarities and differences in the models which we are trying to develop. Furthermore, because the paper is structured in a parallel manner where concepts which vary from one model to another are described one after the other, and concepts which are static to both cases are described only once, it is best to keep the following graphical representation in mind

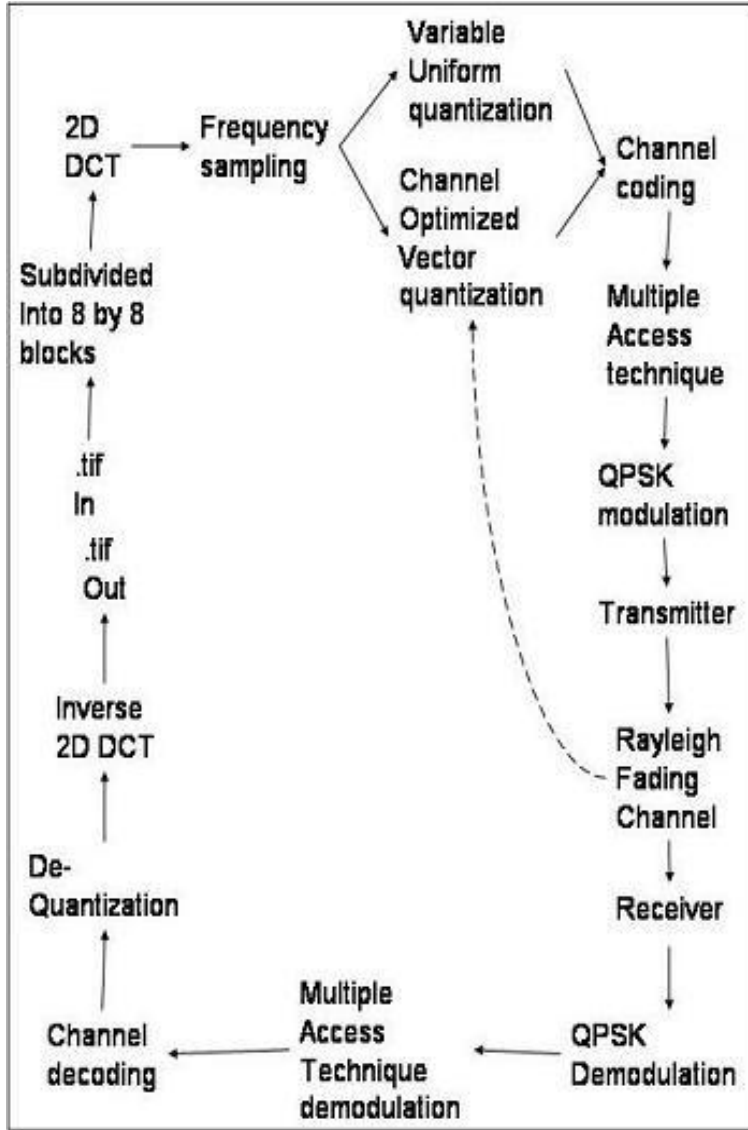


Figure 2.1: Graphical Overview of Simulation

2.3 Mathematical Overview of Proposed Model

In this thesis we explore the possibility of applying a JSCC solution to JPEG transmission of data over Rayleigh fading channels. The physical Rayleigh fading channel is a bandlimited continuous-time channel. We will develop an algorithm based on a COVQ to assign codewords to codevectors of a vector quantizer. As we will review in more detail later in this

section, a vector quantizer is a mapping that assigns to a source output vector

$$x = (x_{nk}, x_{nk+1}, \dots, x_{nk+k-1}) \quad (2.1)$$

a new vector

$$y = q(x) \quad (2.2)$$

that is taken from a finite codebook with a specific partition that outlines the regions that each codebook vector encodes. The performance of a vector quantizer is measured by the average distortion per sample describes as

$$D_s(q) = \frac{1}{k} \sum_{i=1}^M \int_{S_i} p(x) d(x, c_i) dx \quad (2.3)$$

where x is the source vector, c_i is the codevector used to represent the source vector, $d(x, c_i)$ is the non-negative distortion measure, $p(x)$ is the probability density function of the source, and the rate is given by

$$R = \frac{1}{k} \log_2 M, \quad \text{bits/sample.} \quad (2.4)$$

If we assume that the channel is memoryless with finite input and output alphabets expressed as

$$\{0, 1, \dots, M - 1\} \quad (2.5)$$

and express the probability that an index j is received when index i is transmitted

$$P(j|i), \quad i, j = 0, 1, \dots, M - 1. \quad (2.6)$$

Thus the average distortion per sample that is caused by the channel is given by [8]

$$D(q; b) = \frac{1}{k} \sum_{i=1}^M \sum_{j=1}^m P(c_i) P(b(c_j)|b(c_i)) d(c_i, c_j) \quad (2.7)$$

where $P(c_i)$ is the a priori probability of a codeword c_i and $P(b(c_j)|b(c_i))$ is the error probability of the given channel. As we will see later in this chapter, the a priori probability of codewords is obtained from the output of the 2D DCT whose coefficients are distributed according to the Laplacian distribution given by

$$p(F) = \frac{\lambda}{2} e^{-\lambda|f|} \quad (2.8)$$

For this specific thesis we utilize a DS-CDMA communication system transmitting over a Rayleigh fading channel which can be characterized using the Standard Gaussian Approximation given by Lok and Lehnert in [32] as

$$P_e = \frac{1}{2} - \frac{1}{2\sqrt{1 + \frac{N_0}{2E_b\sigma^2} + \frac{2}{3N} [(1 + \frac{M_c}{5}) LK - 1]}} \quad (2.9)$$

where M_c is the number of interfering cells, σ^2 is the variance of the Rayleigh random variable modeling the fading process, L is the number of multipaths per user, K is the number of active users in the system, and $\frac{E_b}{N_0}$ is the bit ratio of bit energy to signal noise.

By substituting the above function in the distortion function given above we obtain

$$D(q; b) = \frac{1}{k} \sum_{i=1}^M \sum_{j=1}^m P(c_i) P_e d(c_i, c_j) \quad (2.10)$$

In order to minimize P_{c_i} in this expression, we must then solve the following mathematical equation

$$\int_{-\infty}^{\infty} \frac{1}{k} \sum_{i=1}^M \sum_{j=1}^m P(c_i) P_e d(c_i, c_j) dc = 0 \quad (2.11)$$

As we can see, the complexity involved in evaluating the above function in order to establish a mathematical expression for our proposed solution is very complex. Hence, to evaluate the validity of our proposed model we opt to perform a simulation. The main theory behind the simulation will be reviewed in the following sub-sections, later we will review the simulation and finally the results and conclusions obtained.

2.4 Source Coding

2.4.1 JPEG

One of the most important topics in image compression technology today is JPEG. The acronym JPEG stands for the Joint Photographic Experts Group, a standards committee that had its origins within the International Standard Organization (ISO).

Historically, the ISO formed the Photographic Experts Group (PEG) to research methods of transmitting video, still images, and text over Integrated Services Digital Network lines in 1982 (ISDN). PEG's goal was to produce a set of industry standards for the transmission of graphics and image data over digital communications networks.

In 1986, CCITT began to research methods of compressing color and gray-scale data for facsimile transmission. The compression methods needed for color facsimile systems were very similar to those being researched by PEG. Hence it was decided that the two groups should combine their resources and work together toward a single standard. Thus in 1987, the ISO and CCITT combined their two groups into a joint committee that would research and produce a single standard of image data compression which was called JPEG.

Before reviewing the specifics behind JPEG, we should briefly mention other types of picture compression techniques available

- GIF images, for example, can store only images with a maximum pixel depth of eight bits. GIF compression has an important set back because of the Lempel Ziv compression algorithm (LZW) which does not work very well on typical image data with low-level noise, such as that commonly found in transmitted images.
- TIFF and BMP, on the other hand, are capable of storing 24-bit data, but in their pre-JPEG versions are capable of using only encoding schemes (LZW and RLE, respectively) that once again do not compress and decompress certain types of image data very well.

JPEG provides a compression method that is capable of compressing continuous-tone image data with a pixel depth of 6 to 24 bits with reasonable speed and efficiency. Furthermore, unlike the other common compression methods described above JPEG is not a single algorithm. Instead JPEG may be thought of as a toolkit of image compression methods which adjusts to fit the needs of the individual users. In other words,

“JPEG may be adjusted to produce very small, compressed images that are of relatively poor quality or very high-quality compressed images that are still far smaller than the original uncompressed data.” [36]

One important difference between JPEG and the other compression techniques is that JPEG is primarily a lossy method of compression, while most popular image format compression schemes, such as RLE, LZW, or the CCITT standards, are lossless. It is important to remember that lossless compression schemes do not discard any data during the encoding process which guarantees that the uncompressed image will be identical to the original image. Lossy schemes, on the other hand, throw useless data away during encoding. JPEG, similar to MPEG, was designed specifically to discard information that the human eye cannot easily see like slight changes in color. On the other hand it retains information which is perceived well by the human eye like intensity (light and dark).

In most lossy compression algorithms such as JPEG and MPEG, the amount of compression achieved depends upon the content of the image data. A typical photographic-quality image may be compressed from 20:1 to 25:1 without experiencing any noticeable degradation in quality. If higher compression ratios are obtained, these will result in image files that differ noticeably from the original image but still have an overall good image quality. By achieving a 20:1 or better compression ratio in many cases not only saves disk space, but also reduces transmission time across data networks and phone lines.

2.4.2 Baseline JPEG

The JPEG specification defines a minimal subset of the standard called baseline JPEG, which all JPEG applications are required to support. In general, the JPEG compression scheme is divided into the following stages

- Sampling of Image (color Images)
- Apply a 2D Discrete Cosine Transform to blocks of pixels.
- Remove redundant image data by setting high frequency coefficients to zero.
- Quantize each block of DCT coefficients.
- Encode the resulting coefficients (image data).

The following figure summarizes these steps, and the following subsections look at each of them in turn. Note that JPEG decoding performs the reverse of these steps, and hence recovers a lossy version of the original image.

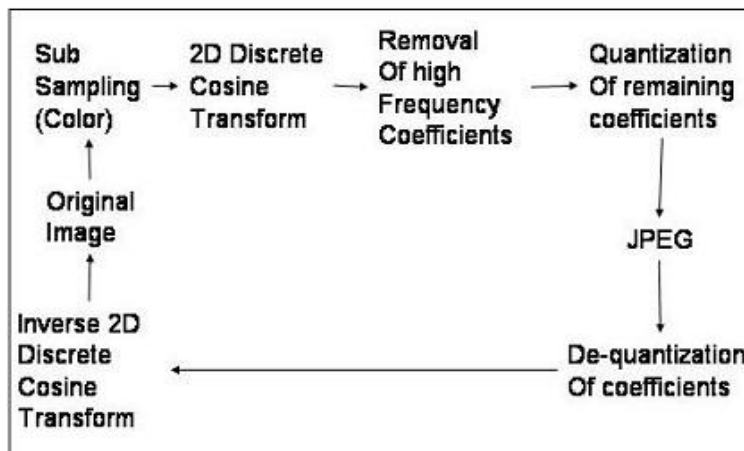


Figure 2.2: JPEG Compression

2.4.3 Sub-Sampling (For Color Images)

Most of the visual information to which human eyes are most sensitive is found in the high-frequency, gray-scale, luminance component (Y) of the YCbCr color space. The other two chrominance components (Cb and Cr) contain high-frequency color information to which the human eye is less sensitive. Most of this information can therefore be discarded.

The simplest way of exploiting the eye’s lesser sensitivity to chrominance information is simply to use fewer pixels for the chrominance channels. For example, in an image whose size is 1000x1000 pixels, we might use a full 1000x1000 luminance pixels but only 500x500 pixels for each chrominance component. In this representation, each chrominance pixel covers the same area as a 2x2 block of luminance pixels. We store a total of six pixel values for each 2x2 block (four luminance values, one for each of the two chrominance channels), rather than the twelve values needed if each component is represented at full resolution. Remarkably, this 50 percent reduction in data volume has almost no effect on the perceived quality of most images. Equivalent savings are not possible with conventional color models such as RGB, because in RGB each color channel carries some luminance information and so any loss of resolution is quite visible.

When the uncompressed data is supplied in a conventional format (equal resolution for all channels), a JPEG compressor must reduce the resolution of the chrominance channels by down sampling, or averaging together groups of pixels. The JPEG standard allows several different choices for the sampling ratios, or relative sizes, of the down sampled channels. The luminance channel is always left at full resolution (1:1 sampling). Typically both chrominance channels are down sampled 2:1 horizontally and either 1:1 or 2:1 vertically, meaning that a chrominance pixel covers the same area as either a 2x1 or a 2x2 block of luminance pixels. JPEG refers to these down sampling processes as 2h1v and 2h2v sampling, respectively [36].

Another notation commonly used is 4 : 2 : 2 sampling for 2h1v and 4 : 2 : 0 sampling for 2h2v; this notation derives from television customs (color transformation and down sampling have been in use since the beginning of color TV transmission). 2h1v sampling is fairly common because it corresponds to the National Television Standards Committee (NTSC), but it offers less compression than 2h2v sampling, with hardly any gain in perceived quality.

Y	U	V
4	2	0
4	2	2

Table 2.1: Sampling of Color Images

2.4.4 Discrete Cosine Transform

In digital systems, continuous time waveforms must be sampled and expressed as a number of discrete samples in order to be adequately interpreted. The Fourier Transform is a technique employed to express an input signal in an equal number of discrete frequencies in which the number of frequency coefficients is equal to the number of input samples. This transformation process is known as a Discrete Fourier Transform.

The Discrete Cosine Transform is a special case of the Discrete Fourier Transform in which the sine components of the coefficients are eliminated leaving a single number. The transformation is done by repeating the samples in a time reversed order and performing a Discrete Fourier Transform on the double length sample set. This process turns the input waveform into an even function whose sine coefficients are all zero.

The DCT is hence similar to the DFT except that all the terms in the expansion are real rather than complex. For an $N \times N$ image block $f(x, y)$, the 2D forward DCT, $F(u, v)$ is given in [5] as follows

$$F(u, v) = \frac{4c(u)c(v)}{N^2} \times \sum_{N-1}^{x=0} \sum_{N-1}^{y=0} f(x, y) \cos \left[\frac{(2x+1)\pi u}{2N} \right] \cos \left[\frac{(2y+1)\pi v}{2N} \right] \quad (2.12)$$

where $N =$ length of one side of the image, $c(u) = \begin{cases} \frac{1}{\sqrt{2}}, & u = 0; \\ 1, & \text{otherwise} \end{cases}$, $c(v) = \begin{cases} \frac{1}{\sqrt{2}}, & v = 0; \\ 1, & \text{otherwise} \end{cases}$, x and y are the pixel coordinates, and u and v are the coefficient coordinates.

The distributions of the coefficients obtained from the 8×8 DCT of natural images has been studied in the context of JPEG. It has been concluded that the generalized Gaussian probability density function (GGF) is a good fit for the AC coefficients resulting from this transformation.

The CGF is characterized by two main parameters: the variance and skewness. When the shape parameter is equal to one, the GGF reduces to a Laplacian distribution, while for a parameter of two it reduces to a normal Gaussian distribution. This shape parameter depends on the image and spatial frequency represented by the coefficients. However, the most common assumption for the distribution of the AC DCT coefficients is Laplacian, which is characterized by the single parameter λ and is given by

$$p(F) = \frac{\lambda}{2} e^{-\lambda|f|} \quad (2.13)$$

The inverse relationship (IDCT) is given by a nearly identical formula which follows

$$f(x, y) = \sum_{N-1}^{u=0} \sum_{N-1}^{v=0} F(u, v) \frac{4c(u)c(v)}{N^2} \cos \left[\frac{(2x+1)\pi u}{2N} \right] \cos \left[\frac{(2y+1)\pi v}{2N} \right] \quad (2.14)$$

These relationships can also be written in matrix form as follows

$$[F]_{N \times N} = [T]_{N \times N} [f]_{N \times N} [T^T]_{N \times N} \quad (2.15)$$

$$[f]_{N \times N} = [T^T]_{N \times N} [F]_{N \times N} [T]_{N \times N} [f]_{N \times N} \quad (2.16)$$

In general, for most images, as u and v increases, the spatial frequency increases and the value of $F(u, v)$ decreases. This means that the DCT returns more insignificant values at higher rather than at lower frequencies. Hence the value of $F(0, 0)$ represents the average value of the whole image or DC value, while the furthest coefficient denoted by $F(N-1, N-1)$ is the coefficient of least importance. since all coefficients except $F(0, 0)$ are AC coefficients, it is possible to set the higher frequency (thus smaller coefficients) to zero which results in a compression of the image.

2.4.5 Quantization

- Variable Uniform Quantization
 - Variable: Defines the step size between quantization values.
 - Uniform: Refers to the fact that each coefficient is quantized individually.

Variable uniform quantization is the main technique of lossy coding as compared to lossless coding. By coarsely quantizing the less significant coefficients in a transform (less significant meaning less noticeable either because the energy is low and/or because it is less visible/audible), the bit rate can be greatly reduced. Typical high quality lossless systems show a bit rate reduction of only 2:1 to 4:1, whereas lossy systems may have reduction ratios of 10:1 to 100:1 or more [35].

Variable uniform quantization can be applied to a complete signal, or more typically, to individual frequency components of a transformed signal. An example of this is JPEG compression, where each individual coefficient resulting from the DCT is quantized.

In the JPEG encoder, variable quantization is applied by means of a quantizing lookup table that provides quantization step sizes and multipliers that scale the DCT coefficients to smaller values. In the JPEG decoder, inverse quantizing is performed by multiplying the recovered coefficients by the inverse step size and scaling factors. The details of the JPEG encoder quantization and codebook will be given in simulation overview section.

- Channel Optimized Vector Quantization

According to the information we just reviewed on JPEG coding, images are transformed into blocks with a 2-dimensional DCT. Each block of 8×8 pixels thus results in a block of 8×8 transform coefficients.

Vector Quantization (VQ) is a lossy data compression method based on the principle of block coding. It is a fixed length algorithm whose design is based on a training

sequence. The use of a training sequence bypasses the need for multi-dimensional integration, a method once used to design the vector subsystem. Hence a VQ that is designed using the training sequence algorithm is referred to as an LBG-VQ, or LVQ, after its creators Linde, Buzo and Gray [19].

Channel Optimized Vector Quantization (COVQ) directly optimizes VQ for a specific channel condition. To do so it introduces information regarding a specific channel into the VQ algorithm. It is important to remember that although a COVQ is optimum for a certain condition, it is most likely sub-optimum under ideal or different conditions. Also, it is important to understand that there are several methods of employing a COVQ. Below we explain one method which uses channel probabilities in the decoder to de-quantize information. However, in our simulation, as seen in the simulation section, we will be using a training codebook channel optimized vector quantization where codevectors are trained to have an optimized decoding region for our specific channel.

In general, given that we have an image subdivided into blocks, where each block contains N pixels, we wish to quantize the block so that $x \rightarrow y_k$. Here y_k are code-words or code-vectors which form a code-book. In this equation, if the number of code-words is k , then the number of bits required to send one vector is $\log_2 k$. Furthermore, if we express k as $k = 2^{NR}$ then for transmission we need NR bits per vector or R bits per pixel.

More specifically, the COVQ design problem can be stated as follows

“Given a vector source whose statistical properties are known, with a given distortion measure and number of code-vectors, find a code-book and a partition which result in the smallest average distortion.” [37]

We assume that there is a training sequence consisting of M source vectors,[9]

$$\tau = \{x_1, x_2, \dots, x_M\} \tag{2.17}$$

The training sequence can be obtained from a large database of pre-established vectors. For example, if the source is a speech signal, then the training sequence can be obtained by recording several long telephone conversations. M can be assumed to be sufficiently large so that all the statistical properties of the source are captured by the training sequence. We assume that the source vectors are k dimensional, or in other words

$$x_m = \{x_{m,1}, x_{m,2}, \dots, x_{m,k}\}, \quad m = 1, 2, \dots, M. \tag{2.18}$$

Let N be the number of code-vectors and let C represents the code-book where C is given by

$$C = \{c_1, c_2, \dots, c_N\} \quad (2.19)$$

Each code-vector is k -dimensional, or can be expressed as

$$c_n = \{c_{n,1}, c_{n,2}, \dots, c_{n,k}\}, \quad n = 1, 2, \dots, N. \quad (2.20)$$

Let S_n be the encoding region associated with code-vector C_n and assume

$$P = \{S_1, S_2, \dots, S_N\} \quad (2.21)$$

denotes the partition of the space. If the source vector x_m is in the encoding region S_n , then its approximation denoted by $Q(X_m)$ is c_n . This can be stated as follows

$$Q(X_m) = c_n, \quad \text{if } x_m \in S_n. \quad (2.22)$$

Quickly restating the overall picture developed by the above equations, the COVQ encoder is specified by a partition of the input space into disjoint encoding regions. Given source vector x_m , index I_{x_m} is transmitted and indicates the encoding region S_n . The decoder receives some index J and produces the corresponding code vector c_J . The overall squared-error distortion measure for the COVQ codebook is given by the following formula

$$D_{ave} = \frac{1}{Mk} \sum_{\forall m} \sum_J P_{J|I_{x_m}} \|x_m - Q(x_m)\|^2 \quad (2.23)$$

In comparison, the overall squared error distortion for a VQ algorithm is given by

$$D_{ave} = \frac{1}{Mk} \sum_{\forall m} \|x_m - Q(x_m)\|^2 \quad (2.24)$$

Here we can clearly see how a COVQ incorporates certain knowledge from the channel into the quantization algorithm.

The overall design problem for either COVQ or VQ can therefore be stated as finding C and P given τ and N , in order to minimize D_{ave} found above. To meet this condition, we observe that C and P must meet the following two criteria

$$S_n = \{x : \|x - c_n\|^2 < \|x - c'_n\|^2\}, \quad \forall n' = 1, 2, \dots, N. \quad (2.25)$$

Which in other words states that the encoding region S_n should consists of all vectors that are closer to c_n than any of the other code-vectors (for those vectors lying on the boundary any tie-breaking procedure will do).

In order to achieve this condition, the code-vector c_n should be average of all those training vectors that are in its encoding region S_n , as stated below

$$c_n = \frac{\sum_{x_m \in S_n} x_m}{\sum_{x_m \in S_n} 1}, \quad n = 1, 2, \dots, N. \quad (2.26)$$

Note: In practice one should ensure that at least one training vector belongs to each encoding region so that the denominator in the above equation is never 0.

Once the code vectors have been constructed, and we have a a fixed encoder $I(x)$ the optimum decoder is given by

$$y_j = \frac{\sum_m x_m P_{J|I_{x_m}}}{\sum_m P_{J|I_{x_m}}} \quad (2.27)$$

which specifies the code vector output.

2.4.6 Entropy Coding

In JPEG, Huffman entropy coding or arithmetic coding is applied to the quantized DCT coefficients. In general, after the coefficients have been adequately quantized and serialized, entropy coding is utilized to represent the resulting information in a compressed manner.

Entropy coding is necessary since the resulting coefficients obtained from the DCT quantization contain a significant amount of redundant data. Huffman or arithmetic compression will losslessly remove the redundancies, ultimately resulting in smaller JPEG data. If arithmetic encoding is used instead of Huffman coding, an even greater compression ratio can be achieved. Below, we will review Huffman entropy coding and arithmetic coding since this is the final step before the JPEG data stream is ready to be transmitted across a communications channel or encapsulated inside an image file format.

- Huffman variable length coding is an entropy code that is optimum in the sense that it achieves the shortest average possible code word length for a source. This average code word length is greater than or equal to the entropy of the source. By entropy we mean a measure of the average information content per source output unit [1]

$$H(s) = \eta = - \sum_i P_i \log(P_i), \text{ bits/symbol.} \quad (2.28)$$

where P_i are the symbol probabilities and H is the theoretical lower bound on the number of bits required to represent a symbol from the source.

The Huffman code is able to achieve compression by allocating short codes to frequent values. Because the codewords produced by an entropy coder are of variable length and are most likely concatenated together and transmitted, it is advantageous that they have the property of being uniquely decodable at the receiver. Hence it is important to avoid prefixes in Huffman coding in order to avoid relying on later values of a bit sequence to decode a received signal and thus also ensure that each code is uniquely decodable.

- The use of an arithmetic coder reduces the resulting size of the JPEG data by a further 10 to 15 percent over the results that would be achieved by the Huffman coder. With no change in the resulting image quality, this gain could be of importance when enormous quantities of JPEG images are archived.

2.5 A Brief Review and Comparison Between JPEG and MPEG Coding

2.5.1 What is MPEG?

MPEG is an acronym that stands for the Moving Pictures Experts Group formed by the International Standards Organization (ISO) to set standards for audio and video compression and transmission. In the following sections we will review the basics behind MPEG coding and review the similarities between it and the previously discussed JPEG compression algorithm.

The first of the techniques developed as a standard for video and audio compression was MPEG1. MPEG1 stored video and audio data at about 1.5Mbps, thus making interactive multimedia systems its primary application. MPEG1 quality can be compared to that of a VHS analog video. In contrast to MPEG1, the applications of audio and video compression encompassed by MPEG2 are limitless and range from high definition images, to electronic cinema, and video phone screens. Audio coding available with the MPEG2 standard stretches from speech grade mono to multichannel surround systems.

2.5.2 JPEG vs MPEG compression algorithms

In a certain way, MPEG can be viewed as a series of JPEG images concatenated together to form a video picture. However, there are very important differences between the compression

algorithm used by JPEG and MPEG, since MPEG must take into account the redundancies that exist between frames in order to encode a minimum set of information based on entropy coding techniques. By doing this, MPEG is able to obtain a compressed version of the original video sequence.

Hence, the differences between MPEG and JPEG coding exist basically because MPEG goes one step further than JPEG to code similarities between different frames, while JPEG obviously does not have different frames. Because of this, we find that both MPEG and JPEG are lossy compression algorithms that break images into 8 by 8 blocks and then depend on the 2D DCT of single images to obtain frequency coefficients of the image.

Besides these similarities, and resembling JPEG where implementation complexity can be varied, MPEG also relies on a trade off between coding performance and complexity to achieved the desired compression.

In more generally terms, it is the type off application desired that defines the type of coding necessary according to the quality of image or video. Lossless coding which retains the quality of the original images, produces a decoded sequence that is identical to the original sequence. In contrast, and similar to JPEG compression, MPEG1 and MPEG2 are both lossy coders that aim to meet a given bit rate maximum for storage and transmission of information.

In a manner that is nearly parallel in comparison to JPEG coding, MPEG explores the correlation between neighboring or nearby pixels by employing a Discrete Cosine Transform (DCT) on image blocks of 8×8 pixels to explore spatial correlation between nearby pixels within an image. However, when correlation between pixels is high, as with two consecutive frames, it is desirable to use inter frame DPCM techniques employing temporal prediction to analyze them. Hence MPEG can be viewed as a hybrid of temporal motion prediction followed by transform coding using hybrid DPCM, DCT coding of video.

As a result, and foreseeing positive results from the simulation which we are designing, it is reasonable to expect that a similar result could be obtained by applying a similar joint source channel coding technique to an MPEG based delivery of digital video over CDMA wireless networks [30].

2.6 Channel Coding

Noise, present in all real channels, is inevitable and leads to the corruption of transmitted information. In the previous section we reviewed source coding and the compression of information using various techniques ultimately aimed at avoiding redundancy. Channel coding on the other hand is the insertion of controlled redundancy into data streams in order to detect and correct errors introduced by the channel. This added redundancy implies an increase in bandwidth and thus an increased complexity in the communication system. If the bandwidth cannot be increased due to physical limitations of the transmission system,

this implies that the source rate would have to be decreased or redundancy eliminated.

In general, there are many types of error correction codes available for use in communication systems which can be grouped in two main sets, convolutional codes and block codes. Convolutional codes are produced when the original information bits are convolved with the impulse response of an encoder. The convolutional operation implies that each encoded output is dependent on the length of the impulse sequence. On the other hand, block codes are formed by taking words k bits long and generating a codeword n bits long, with $n > k$. In this situation the extra $n - k$ bits are related to the original k bits by an algebraic formula.

Furthermore, when the channel over which we are transmitting is a busy channel, such as in wireless communications, then there exists the possibility that the channel code may not perform optimally when bursts occur within our channel. In order to overcome this problem we may use an interleaver which is a device that mixes up symbols from different codewords so that consecutive symbols within the same code word are spread across several codewords. Hence when the new code is sent across a busy channel, bursts affect symbols from different codewords. The effect of the interleaver is thus to randomize the burst errors seen by the channel decoder.

However, because this thesis is trying to evaluate the effect of the channel on our compression scheme we will not be using any channel coding and no redundancy will be coded into the data in order to obtain more appreciable results.

Our simulation will consist of the transmission of the original source coded information which will determine the measure of our success in jointly coding the source and channel by using alternate methods of quantization in contrast to the proposed methods used in JPEG compression.

2.7 Access Technique: CDMA

CDMA, the acronym that stands for Code Division Multiple Access, has recently become one of the standards for information transfer in the mobile communication community. The key property that has made CDMA increasingly popular is that it has the unique capability of sustaining multiple users over a given frequency channel by employing the concept of orthogonal waveforms sometimes also referred to as orthogonal code words. In general the orthogonality concept allows a multitude of separate different data streams to be simultaneously transmitted over the same frequency channel. The following quotation taken from [23] briefly summarizes what CDMA is

“CDMA is a multiple access technique where low correlation or orthogonal codewords are used to separate a multitude of different data streams simultaneously transmitted over the same channel. Hence CDMA utilizes code diversity as a method of separating one simultaneous data stream from another.”

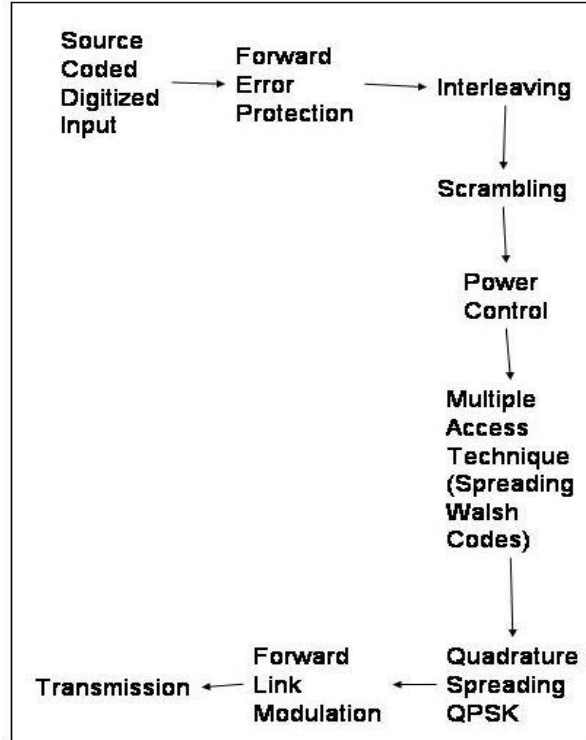


Figure 2.3: Available Channel Coding Techniques

Today’s CDMA wireless networks are based on Direct Sequence Spread Spectrum (DSSS), a technique where information is transmitted in the same frequency range and with the same bandwidth for different users with the subtle exception that each signal is assigned a coding sequence which identifies it. To further understand DS-CDMA we must thus review the concept behind Spread Spectrum Communication.

2.7.1 What is Spread Spectrum Communication?

Spread Spectrum Communication is often defined as

“A means of communication where the transmitted signal occupies a bandwidth in excess of the minimum required bandwidth to successfully send the information. This bandwidth spreading is accomplished by means of a unique code which is independent of the transmitted data, and a synchronized reception with the unique spreading code at the receiver is used for de-spreading and subsequent data recovery.” [18]

In other words Direct Sequence Spread Spectrum is a spreading that happens when the spectrum of a data signal is spread by a faster pseudo-randomly generated sequence, which

causes phase transitions in the carrier signal containing the transmitted data. The spreading is performed by a direct multiplication in the time domain of each symbol or data bit by an unique chipping code. The resulting signal obtains what is known as the Process Gain, or a gain in bandwidth. The following figure depicts an example of spreading in a simple DS-CDMA transmitter where the unique codeword, or PN code, acts as the DS spreading chip code.

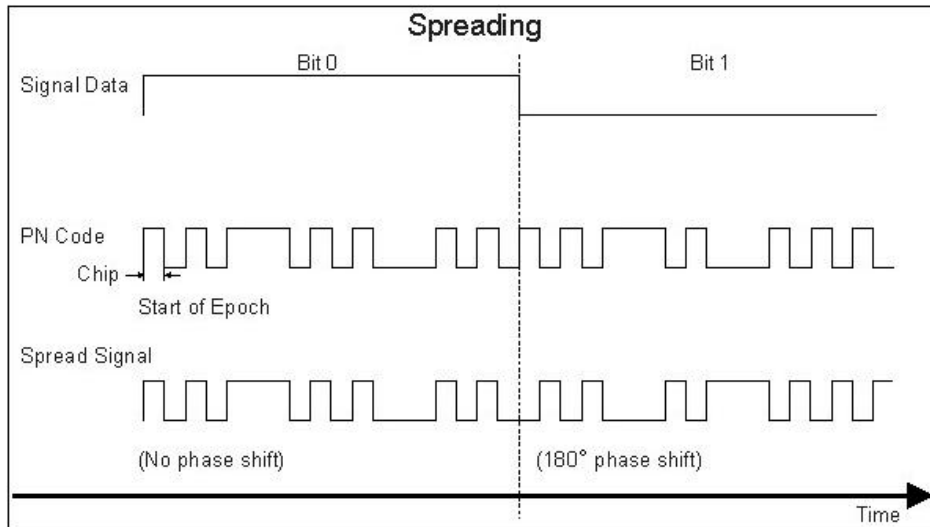


Figure 2.4: DS-CDMA Spreading Technique

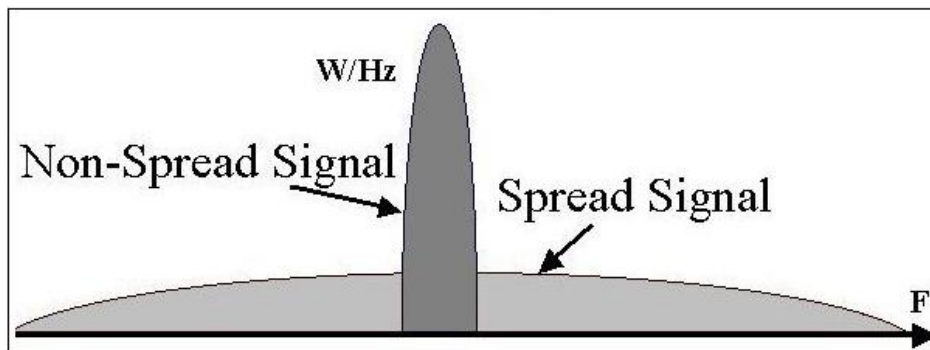


Figure 2.5: DS-CDMA Spreading of Signal

Briefly restating what was previously mentioned, DS-CDMA works by taking a data sequence and spreading it across the spectrum after being encoded by spreading codes, each of which is assigned uniquely to each user at a higher rate than the symbol rate of the information data. The spread high-speed data sequence is referred to as a chip and the rate

at which the spread data varies is called chip rate. By taking the ratio of chip rate to symbol rate we obtain the Spreading Factor (SF). At the destination, the same spreading code is utilized to perform correlation detection, also referred to as despreading, in order to recover the transmitted data sequence. Because signals received by other users carry the different spreading codecs, the signal power is reduced evenly to $\frac{1}{SF}$. Now, assuming that $d_k(t)$ and $c_k(t)$ are user k 's data modulation waveform and spreading signal waveform, respectively, we can represent these two parameters in the following way

$$d_k(t) = \sum_{\infty}^{i=-\infty} b_k(i) \cdot u\left(\frac{t}{T_s} - i\right) = \sum_{\infty}^{i=-\infty} e^{j\phi_k(i)} \cdot u\left(\frac{t}{T_s} - i\right) \quad (2.29)$$

$$c_k(t) = \sum_{\infty}^{i=-\infty} p_k(i) \cdot u\left(\frac{t}{T_s} - i\right) \quad (2.30)$$

In the above equations T_s and T_c represent the symbol length and chip length respectively, $SF = \frac{T_s}{T_c} \cdot u(t)$, and $p_k(i)$ is a binary spreading code sequence and $b_k(i)$ is an encoding information data sequence.

By assuming that the data modulation phase is Quadrature Phase Shift Keying (QPSK) then we can set $\phi(i) \in \{j\frac{\pi}{2} + \frac{pi}{4}; j = 0, 1, 2, 3\}$.

Briefly introducing the transmission channel, and taking into consideration that it is a mobile multipath Rayleigh fading channel generated because of variations in transmission time caused by obstructions between the base station and the mobile station we can introduce a preliminary mathematical approximation $r(t)$ of the received signal as

$$r(t) = \sum_{K-1}^{k=0} \sqrt{2S_k} \sum_{L_k-1}^{l=0} \xi_{k,l}(t) c_k(t - \tau_{k,l}) + w(t) \quad (2.31)$$

where S_k represents the transmission power of user k , and $\xi_{k,l}$ and $\tau_{k,l}$ stand for the complex channel gain or fading complex envelope of user k 's path l ($l = 0, \dots, L_k - 1$) and delay time respectively. Furthermore, in the above equation it is assumed that $E\left[\sum_{L_k-1}^{l=0} |\xi_{k,l}(t)|^2\right] = 1$, in which $E(\cdot)$ represents the ensemble mean. Finally, $w(t)$ is the Gaussian noise portion of the power spectrum density $\frac{N_0}{2}$. Further detail of the Rayleigh fading channel will be reviewed further in other sections.

Advantages of a wireless communication system based on DS-CDMA

- Soft Hand off Capabilities:

Because CDMA is a digital communication technique, any given transmitter can communicate simultaneously with multiple stations thus giving the system a soft hand of capability when moving from one cell to another.

- Capacity Increase for Wireless Technologies:
Because CDMA allows multiple users to utilize the same frequency, existing communications networks can be enhanced to allow more users to share the same frequency spectrum allocated for the existing system.
- Digital Service:
CDMA networks are based on digital rather than analog delivery of information which gives the user a larger range of services.
- Reduced transmitted power.
- Reduced incidence of dropped calls.

2.8 Frequency Modulation

Before we begin to talk about frequency modulation we should briefly review what we have seen up to this point

- First the .tif image is converted into .jpeg image (Source Coding).
- The information is then quantized and serialized for transmission (Source Coding).
- Redundancy is inserted into the coded information (Channel Coding if applied).
- The information is finally coded using access technique (CDMA).

As reviewed, the digital bit stream that is going to be transmitted passes through a set of stages which aim at making the information statistically more robust for a given channel. Once this has taken place, the data is modulated onto a radio frequency carrier. Typically CDMA networks work with either an 800MHz carrier frequency or a 1900MHz carrier frequency. The modulation of a signal onto a radio frequency is important to meet frequency transmission specifications and decrease antenna transmission size among other important factors.

2.8.1 QPSK Modulation

The digital bit stream in CDMA wireless communications networks is modulated onto a radio frequency (RF) carrier in order to be transmitted. Modulation is necessary in order to transmit at a frequency specified by the government, which in the case of mobile communication systems is often 800MHz. For CDMA systems the standard modulation is Quadrature Phase Shift Keying (QPSK). QPSK makes use of the quadrature components and the in-phase components as follows.

If we denote the in-phase and quadrature data waveforms as $d_c(t)$ and $d_s(t)$ respectively, and the corresponding pseudo random noise binary waveforms as $c_c(t)$ and $c_s(t)$, then the QPSK signal can be represented using the following equation [27]

$$x(t) = c_c(t)d_c(t)\sqrt{S}\cos(w_c t) + c_s(t)d_s(t)\sqrt{S}\sin(w_c t) \quad (2.32)$$

where: $d_c(t)$ = in phase waveform, $d_s(t)$ =quadrature data waveform, $c_c(t)$ & $c_s(t)$ = pseudo random noise binary waveforms, S = signal power, and w_c = carrier frequency.

If we compare this equation to the one employed by Coherent Binary Phase Shift Keying, we can clearly see how QPSK employs orthogonal wave forms to double the capacity of the channel

$$x(t) = c(t)d(t)s(t) = c(t)d(t)\sqrt{2S}\cos(w_c t) \quad (2.33)$$

where $s(t) = \sqrt{2S}\cos(w_c t)$, $d(t)$ = baseband signal at the transmitter input and receiver output, $c(t)$ = spreading signal, S = signal power, and w_c = carrier frequency.

In general, QPSK is the combination of two BPSK systems, thus doubling the effective bandwidth efficiency of the channel by transmitting an additional bit during the period of transmission T .

2.9 Filtering

An important problem with QPSK is that the spectrum is not compact enough to realize data rates approaching the radio frequency (RF) channel bandwidth (BW). Information that is transmitted using QPSK has large frequency sidelobes. For wireless data transmission systems which require efficient use of the RF channel BW, it is necessary to reduce the energy of the QPSK upper sidelobes. A straightforward means of reducing this energy is to lowpass filter the data stream prior to transmission. The lowpass filter must have a narrow BW with a sharp cutoff frequency and very little overshoot in its impulse response. This is where the Nyquist filter characteristic come in.

Nyquist filters are characterized in the time-domain by their impulse response being exactly equal to zero every L samples (except the exact middle sample of the impulse response). This is precisely why we get a sub filter that is a perfect allpass delay and allows the samples to be interpolated to pass through the filter unchanged.

Further characteristics of the filter designed for our simulation will be reviewed in section [4] of this paper.

2.10 Channel Type

Research on aspects of wireless communications related to consumer applications has been active for at least the last thirty years. In 1970, the FCC made available a 75 MHz band

in the 806-881 MHz range for mobile telephony. This relatively large capacity system paved the way for significant innovations in cellular networks, personal communications services and more recently for data services on wireless networks.

The evolution of the wireless networks is often captured in terms of first (1G), second (2G) and third (3G) generation systems. The first generation systems describe the analog systems that are based on frequency-division multiple access (FDMA). In cellular systems this division was defined as the Advanced Mobile Phone System (AMPS) in the United States, as Nordic Mobile Telephony (NMT) in the European Nordic countries and the Nippon Telephone and Telegraph (NTT) system in Japan. The AMPS system, for example, supports 832 channels at 30 KHz carrier spacing. The 2G systems that evolved from the mid to late eighties focused on digital modulation techniques and time-division multiple access (TDMA) schemes.

The advent of the world-wide-web (WWW) and commercialization of the Internet during the mid nineties set the tone for expected functionality of the third generation systems. Wireless communication no longer meant mobile plain voice telephony service. Wireless services are expected to include voice mail, e-mail, instant messaging, multimedia messaging, web and intra net access. These services are to be supported on digital devices such as cellular phone, PDA, the personal computer and its peripherals. Spread spectrum technology on which CDMA is based was considered as the most viable means of achieving the higher data rates required for multimedia wireless transmission. However, 3G standards based on the GSM TDMA model are also being considered.

Most, if not all of the aforementioned standards activities have focused on the support of enhanced mobile telephony services such as the ones being explored throughout this thesis. It is clear from our discussion that not all the advances in wireless communications were oriented towards telephone services. In the last five years, for example, the demand for fixed wireless systems has arisen, particularly in the context of setting up mobile networks for various consumer and business related applications. The concept of the wireless local area network (WLAN) is extremely important. The application of WLANs may be found in campus offices, small office, home office, hospitals, residences, warehouses, manufacturing facilities, parking lots, building-to-building complexes and limited outdoor regions. In the last two years, major computer and telecommunication systems providers have developed cost effective wireless terminal cards and access points for deploying WLANs in the industrial, scientific and medical (ISM) frequency bands in the 902-928, 2400-2483.5 MHz and 5.725-5.825 GHz ranges. The FCC allows operation of low-power spread spectrum (SS) devices in these frequency bands.

2.10.1 Important Radio Channel Characteristics

Radio waves that are transmitted from a base station radiate in all directions. The receiver's observer collects these radio waves, including reflected waves, diffracted waves, and scattered waves, which reach the mobile station at different times and causes the phase of the incoming waves to vary. This environment is known as a multipath propagation environment where the received signal is sometimes intensified or weakened by the superposition of different waves, effect known as multipath fading.

When considering multipath wireless channels there are several other characteristics that should be reviewed and which are closely linked with multipath propagation. Specifically these parameters are the *time delay spread*, *coherence bandwidth*, *Doppler Spread* and the number of *Resolvable Paths*. These parameters are all reviewed next.

T_{delay} is a measure of the length of the impulse response for the multipath wireless channel. The Time Delay Spreads leads to inter-symbol interference and thus degrades the performance of the wireless communication system ultimately complicating the receiver design. Many times the impulse response is characterized by its root mean square time delay spread, $T_{delay_{rms}}$, defined as the standard deviation of the channel's power delay profile. Specifically, for the wireless indoor channel, the value of $T_{delay_{rms}} = 10 - 60ns$. Another way of characterizing the time delay of a system is by using its maximum value, or maximum Time Delay Spread $T_{delay_{max}}$. This value is determined by the range of delays over which the delay peaks of the channel power delay profile is not less than 30 dB from the peak of the first received pulse. If we take this definition of time delay into consideration, experiments have shown that for communication systems whose frequency ranges between 850MHz up to 4GHz experience a $T_{delay_{max}} = 270 - 300ns$.

The $B_{coherence}$ or Coherence Bandwidth is directly related to the time delay spread. In general, the $B_{coherence}$ can be expressed by the following equation, as noted in [14]

$$B_{coherence} = \frac{1}{2\pi T_{delay}} \quad (2.34)$$

When frequencies lie within the coherence bandwidth they are likely to experience correlated fading. The resulting channel can be described as frequency non-selective where all the frequency components are subject to the same attenuation, phase shift and time delay this is usually the case for narrow band wireless channels.

The doppler spread, interpreted as the variation of the shift in the carrier frequency, can be viewed more intuitively as the measure of the rate at which the channel changes. In general we can relate small Doppler spreads to large coherence times, $T_{coherence}$ or slowly changing channels. For these channels, given an omni directional vertical antenna $\frac{\lambda}{4}$ with an azimuthal gain $G(\alpha)$ and uniform power distribution $p(\alpha) = \frac{1}{2\pi}$ over 0 to 2π we can express the doppler power spectrum as follows

$$PSD_{Doppler}(f) = \frac{G(\alpha)}{\pi f_m \sqrt{1 - \left(\frac{f-f_c}{f_m}\right)^2}} \quad (2.35)$$

where f_m is the maximum Doppler shift and f_c is the carrier wave frequency of the wireless mobile communication system.

It is important to note that if a wireless communication symbol duration, T_{symbol} , is large in comparison to the coherence time, then the wireless channel is subject to fast fading. The following table, taken from [25], helps us relate different multipath characteristics with different channel models and operation environments.

Channel Characteristics	$T_{symbol} \ll T_{coherence}$	$T_{symbol} \gg T_{coherence}$	Channel Model
$B_{symbol} \ll B_{coherence}$	Non-dispersive, flat-flat fading	Time-Dispersive, frequency-flat fading	Frequency non selective fading (narrow band)
$B_{symbol} \gg B_{coherence}$	Frequency-dispersive, time-flat	Doubly (time and frequency) dispersive	Frequency selective fading (Wideband)
Operational Environment	Slowly fading (Indoor channel)	Fast fading (Outdoor Channel)	

Table 2.2: Multipath Channel Characteristics, Models, and Operational Environments

The last important characteristic we wish to mention is the number of resolvable paths in a multipath wireless channel which can be defined as follows

$$R_{path} = \left\lceil \frac{T_{delay_{max}}}{T_{symbol}} \right\rceil + 1 \quad (2.36)$$

In narrow band communication systems there is usually only one resolvable path since $B_{coherence} \gg B_{symbol}$. It is important to note that for all real multipath wireless channels the number of resolvable paths is a random variable, however, for simplicity we will assume that the approximation given by R_{path} is correct.

2.10.2 Characteristics of the Indoor Wireless Channel

As described previously, an indoor wireless channel is characterized by the transmitted signal decomposing into multiple copies of the original signal. This decomposition occurs due to

multiple path reflections of the surrounding environment. More specifically, in an indoor environment we may expect obstacles such as business machines and furniture to weaken the signal. In order to adequately comprehend indoor propagation it is thus important to look at reflections, scattering and diffraction in this type of environment. The following are the basic definitions for these three parameters which are fundamental in understanding a wireless environment [25].

- **Reflections:**
Occur when a propagating electromagnetic wave is incident on a large object in comparison to the wavelength of the propagating wave. When reflection occurs on transparent media it is also important to note that part of the electromagnetic wave is reflected while the rest is transmitted through to the second medium. This effect, or bending is referred to as refraction.
- **Scattering:**
Another multipath channel effect occurs when the medium in which the electromagnetic wave travels contains objects whose dimensions are small compared to the electromagnetic wavelength, and the number of objects in the medium is large. Some objects which might cause scattering, for example, are smoke, carpet, and plants.
- **Diffraction:**
Diffraction occurs when the path between the transmitter and the receiver is obstructed by surfaces with irregularities. The resulting wavefronts, as explained by Huygen's principle, bend around obstacles before reaching their destination.

Overall, once the received information has reached the receiver it consists of the superposition of multiple wave fronts that may add up constructively or destructively and interfere with each other creating an obstacle for data transmission in a wireless channel.

2.10.3 Indoor Propagation Models

Once personal communication systems appeared on the market, there was a lot of interest to characterize and operate controlled radio channels within buildings, thus a characterization of radio propagation inside buildings has to be developed. In general, the indoor radio channel differs from traditional mobile communications in various aspects [25].

- The distances covered are much smaller.
- The variability of the environment is much greater for a smaller range of transmission-reception separation distances.

Material Type	Loss(dB)	Frequency
All metal	26	815MHz
Aluminum siding	20.4	815MHz
Foil insulation	3.9	815MHz
Concrete block wall	13	1300MHz
Light machinery <10sqft	1-4	13000MHz
General machinery 10-20sqft	5-10	1300MHz
Heavy machinery >20sqft	10-12	1300MHz
Concrete wall	8-15	1300MHz
Concrete floor	38	1300MHz
Metal catwalk/staris	5	1300MHz
Empty cardboard inventory boxes	3-6	1300MHz

Table 2.3: Average Signal Loss Measurements for Radio Paths Obstructed by Common Building Materials

- The building type, construction materials, layout and other specific features greatly affects the propagation within buildings.

Similar to conventional radio communications, indoor channels can be classified as either line-of-sight (LOS) or obstructed (OBS). Also, the amount of obstruction, or cluttering between the receiver and transmitter may vary greatly. Below we will review a few of the models which have been developed, and specify which specific model we will be utilizing for this model [25].

- Partition Losses (Same floor):

Structures in distinct geographical regions are built differently to withstand natural disasters, heat, snow, wind, etc. One of the most common models to describe partitions and obstacles within the same floor takes into account wood framing partitions with plaster board and internal walls made of wood or non reinforced concrete. To differentiate the two kinds of partitions we call partitions formed as part of the building structure as hard partitions, and partitions that are movable and which do not span to the ceiling soft partitions. In efforts to classify partitions researchers have formed extensive data bases of losses for many different types of partitions, the most important are named in table 2.3.

- Partition Losses (Between floors):

The losses between floors of a building are also dependent of the dimensions

and materials used to construct the building, even factors like the amount of windows in a building and the presence of tinting can impact the loss between floors. The following table displays measurements are examples of losses that can be expected between floors. The data is taken from the San Francisco PacBell building

Number of Floors	Average Loss(dB)	Frequency
One floor	13.2	915MHz
Two floors	18.1	915MHz
Three floors	24.0	915MHz
Four floors	27.0	915MHz
Five floors	27.1	915MHz

Table 2.4: Average Signal Loss Measurements for Radio Paths Obstructed by Floor Separations

- Log-Distance Path Loss Model:

One mathematical approximation that has been developed and which has been shown to approximate the indoor path loss is the log distance model whose equation is

$$PL(dB) = PL(d_0) + 10n \log\left(\frac{d}{d_0}\right) + X_\sigma \quad (2.37)$$

where the value of n depends on the surroundings and building type, X_σ is a normal random variable expressed in dB having a standard deviation of σdB . Some values that are typically used when using this approximation are the following.

Building	Frequency (MHz)	n	$\sigma(dB)$
Office, soft partition	900	2.4	9.6
Retail stores	914	2.2	8.7
Suburban Home Indoor street	900	3.0	7.0

Table 2.5: Average Signal Loss Measurements for Radio Paths Obstructed by Common Building Materials

2.10.4 Multipath Fading Radio Channel Model: Rayleigh Fading Model

A common model used to describe multipath fading radio channels characterized by narrow band fading and indoor environments is the Rayleigh fading model. The Rayleigh fading

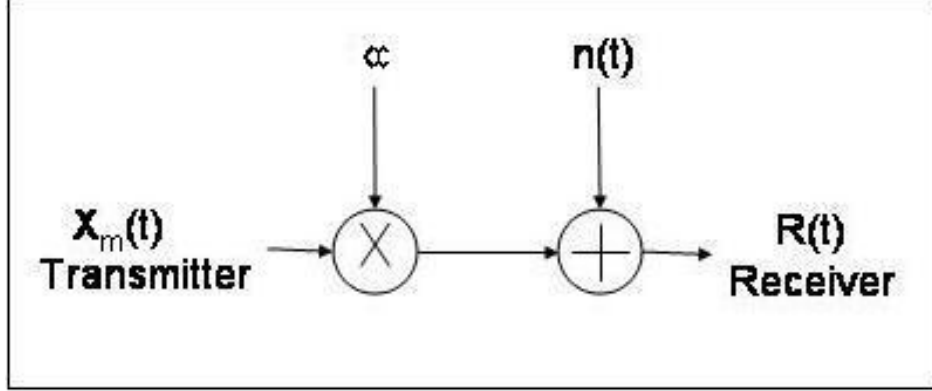


Figure 2.6: Rayleigh Fading Channel Model $r(t) = \alpha x_m(t) + n(t)$

model is appropriate for situations in which the composite received signal consists of numerous signal paths, R_{path} where $R_{path} > 6$. In this case, and according to the central limit theorem, the received complex low pass signal can be described by the following equation

$$r(t) = r_I(t) + jr_Q(t) \quad (2.38)$$

Hence we can model $r(t)$ as a complex random Gaussian process. In the case when there is no line of sight the random variables r_I and r_Q would have zero mean and hence the received complex envelope denoted by $z(t)$ would be equal to the magnitude of $r(t)$

$$z(t) = |r(t)| \quad (2.39)$$

and would have a Rayleigh distribution at any time t as the probability density function describes

$$P_R(r) = \frac{r}{\sigma^2} e^{-\frac{r^2}{2\sigma^2}} \quad (2.40)$$

The corresponding cumulative density function of the Rayleigh distribution, obtained by integrating the probability density function, would then be given by

$$F_R(r) = 1 - e^{-\frac{r^2}{2\sigma^2}}, \quad r \geq 0. \quad (2.41)$$

The mechanism by which fading occurs is when a wave is incident with angle θ_n on an object. The delayed wave is given by

$$r_n(t) = Re[e_n(t)e^{j(2\pi f_c t)}] \quad (2.42)$$

where $Re[]$ indicates the real part of a complex number that gives the complex envelope of the incoming wave from the direction of the number n . $e_n(t)$ in this equation is given by

using the propagation path length from the base station of the incoming waves($L_n(m)$), the speed of mobile station ($v(m/s)$), and the wavelength ($\lambda(m)$)

$$e_n(t) = R_n(t)e^{j(\frac{2\pi(L_n-vt\cos\theta_n)}{\lambda}+\phi_n)} = x_n(t) + jy_n(t) \quad (2.43)$$

R_n is the envelope of the n-th incoming wave, ϕ_n is the phase of the incoming wave, $x_n(t)$ is the in-phase factor of $e_n(t)$, and $y_n(t)$ is the quadrature-phase factor of $e_n(t)$.

Where the $n - th$ incoming wave shifts the carrier frequency by the doppler effect, also known as the doppler shift f_d in land mobile communications, the shift may vary depending on the angle of motion with respect to the transmitting antenna position.

Because the received wave in the mobile station is a synthesis of the above, then we can derive the following expression when the wave number is made to be N

$$r(t) = \sum_{n=1}^N r_n(t) = Re \left[\left(\sum_{n=1}^N e_n(t) \right) e^{j(2\pi f_c t)} \right] \quad (2.44)$$

$$r(t) = Re [(x(t) + jy(t))(\cos(2\pi f_c t) + jsin(2\pi f_c t))] \quad (2.45)$$

$$r(t) = x(t)\cos(2\pi f_c t) - y(t)\sin(2\pi f_c t) \quad (2.46)$$

where $x(t)$ and $y(t)$ are normalized random processes having an average value of 0 and dispersion of θ given that N is large enough, and can be expressed as follows

$$x(t) = \sum_{n=1}^N x_n(t) \quad (2.47)$$

$$y(t) = \sum_{n=1}^N y_n(t) \quad (2.48)$$

Using the following formula for the combined probability density function $p(x, y)$

$$p_{x,y}(x, y) = \frac{1}{2\pi\sigma^2} e^{-\frac{x^2+y^2}{2\sigma^2}} \quad (2.49)$$

and expressing x and y in terms of amplitude and phase of a received wave thus transforming the above equation into $p(R, \theta)$ given by

$$p_{R,\theta}(R, \theta) = \frac{R}{2\pi\sigma^2} e^{-\frac{R^2}{2\sigma^2}} \quad (2.50)$$

The marginal probability density function $p(R)$ can then be obtained by integrating $p(R, \theta)$ over θ which yields the following

$$p(R) = \frac{R}{2\sigma^2} e^{-\frac{R^2}{2\sigma^2}} \quad (2.51)$$

Similarly we can integrate over R to obtain the probability density function $p(\theta)$ as follows

$$p(\theta) = \frac{1}{2\pi} \quad (2.52)$$

We can thus deduce from the above equations that R and θ are independent from each other. Furthermore, the envelope fluctuation follows a Rayleigh distribution, and the phase fluctuation follows a uniform distribution.

In order to simulate the Rayleigh fading environment we take into consideration that the mobile station receives the radio wave at different angles which are uniformly distributed, and the wave number of the incoming waves is N . For this case, the complex fading fluctuation can be given by

$$r(t) = x(t) + jy(t) \quad (2.53)$$

or in other words we can express $r(t)$ as follows

$$r(t) = \left[\sqrt{\frac{2}{N_1+1}} \sum_{n=1}^{N_1} \sin\left(\frac{\pi n}{N_1}\right) \cos\left(2\pi f_d \cos\left(\frac{2\pi n}{N_1}\right)t\right) + \dots \right. \\ \left. \frac{1}{\sqrt{N_1+1}} \cos(2\pi f_d t) \right] + j \sqrt{\frac{2}{N_1}} \sum_{n=1}^{N_1} \sin\left(\frac{\pi n}{N_1}\right) \cos\left(2\pi f_d \cos\left(\frac{2\pi n}{N_1}\right)t\right)$$

Another important aspect of the multipath propagation environment is that the mobile station receives the direct, reflected and scattered waves which are related with each other in various ways. From the above discussion it is clear that the amplitude has a Rayleigh distribution and that the phase has a uniform distribution when we observe the received signal at the arrival time. Hence we may assume that there are fixed ratios of average electric powers of the direct and delayed waves. By giving the relative signal level and relative delay time of each delayed wave in comparison with the direct wave we are therefore able to recreate the multipath propagation environment.

2.10.5 BER Approximations for DS-CDMA Communications Systems over Rayleigh Fading Channels

The standard Gaussian approximation and Holtzman's Gaussian approximation to accommodate for quadriphase modulated DS-CDMA communications systems over an AWGN channel is given by Lock and Lehnert as

$$P_e = Q \left(\sqrt{\frac{L}{\bar{V} + L \frac{N_0}{2E_b}}} \right) \quad (2.54)$$

and the Holtzman's approximation as

$$P_e = \frac{2}{3}Q\left(\sqrt{\frac{L}{\bar{V} + L\frac{N_0}{2E_b}}}\right) + \frac{1}{6}Q\left(\sqrt{\frac{L}{\bar{V} + 3\sqrt{3}\sigma_v + L\frac{N_0}{2E_b}}}\right) + \frac{1}{6}Q\left(\sqrt{\frac{L}{\bar{V} - 3\sqrt{3}\sigma_v + L\frac{N_0}{2E_b}}}\right) \quad (2.55)$$

where \bar{V} and σ_v^2 are the means and variance of V for different kind of channel modulation schemes as given in the following table

Modulation	$\frac{\bar{V}}{N-1}$	$\frac{\sigma_v^2}{N-1}$
QPSK	$\frac{2}{3}$	$\frac{1}{45}$
OQPSK	$\frac{2}{3}$	$\frac{17}{1440}$
MSK	$\frac{15+2\pi^2}{6\pi^2}$	$\frac{-16830+1842\pi^2+77\pi^4}{2304\pi^4}$

Table 2.6: Mean and Variance for Different Modulation Schemes

The preceding approximations can be extended to a DS-CDMA system over a Rayleigh fading channel, as reviewed previously in section [2.3] and explained in [32], as follows

$$P_e = \frac{1}{2} - \frac{1}{2\sqrt{1 + \frac{N_0}{2E_b\sigma^2} + \frac{2}{3N} \left[\left(1 + \frac{M_c}{5}\right) LK - 1 \right]}} \quad (2.56)$$

where M_c is the number of interfering cells, σ^2 is the variance of the Rayleigh random variable modeling the fading process, L is the number of multipaths per user, K is the number of active users in the system, and $\frac{E_b}{N_0}$ is the bit ratio of bit energy to signal noise.

3 Joint Source Channel Code Design

In the background information reviewed above we have gone over the material necessary to understand the simulation that will follow. The next two paragraphs briefly re-state our original hypothesis:

As is, the original JPEG compression and transmission scheme quantizes each individual coefficient as dictated by a specific table. The resulting quantization does not contain any information relative to the specific channel which is being studied and hence results in a sub-optimal coding technique for a Rayleigh fading channel.

In this thesis we propose a joint source channel code design, as reviewed earlier, to improve this design by replacing the present method of quantization by a channel optimized vector quantizer (COVQ). By using a COVQ we can incorporate specific information regarding the channel into the quantization scheme of the source by constructing an adequately trained set of codebook vectors.

In the following section, Simulation Overview, we will review the simulation used to test our hypothesis in detail. Once again, we will be adopting an organizational scheme similar to the one followed by this thesis, where concepts that differ from one simulation to the other are reviewed one after the other, and all common concepts are reviewed in the order in which they are called upon in the simulation.

4 Simulation Overview

In order to perform this simulation we will be using both a Matlab programmed JPEG encoder, and a Matlab CDMA 800MHz wireless transmission model. Also to explain the simulation, we will review both the normal and improved algorithms in a parallel manner to avoid redundancy.

The following bullets describe the main functions and sub functions in both simulations and provides an outline of the description that follows.

- .tif to .jpg conversion:
For the JPEG encoding and decoding process we will be using a basic Matlab programmed JPEG encoder decoder
- Quantization:
Quantization will be described in two sub-blocks. The first subsection will describe Lloyds Variable Uniform Quantization and in the second subsection we will review the LVQ approach to quantization
- Decimal to binary:
Once quantization has taken place, coefficients are transformed to binary using arithmetic coding.
- Transmission of data:
 - QPSK modulation
 - The CDMA access technique
 - The transmission of the encoded image through a wireless Rayleigh fading channel
- Receiver
- Binary to decimal
- De-Quantization of received coefficients
- JPEG decoding

Further, it is also important to keep in mind the mathematical function developed in section [2.3] which stated

$$D(q; b) = \frac{1}{k} \sum_{i=1}^M \sum_{j=1}^m P(c_i) P_e d(c_i, c_j) \quad (4.1)$$

$$P_e = \frac{1}{2} - \frac{1}{2\sqrt{1 + \frac{N_0}{2E_b\sigma^2} + \frac{2}{3N} \left[\left(1 + \frac{M_c}{5}\right) LK - 1 \right]}} \quad (4.2)$$

remembering that $\frac{1}{k}$ makes reference to the symbol rate, $P(c_i)$ to the probability of transmitting a specific index from the codebook alphabet, $\frac{E_b}{N_0}$ is the bit over noise ratio, M_c is the number of interfering cells, σ^2 is the variance of the Rayleigh random variable modeling the fading process, L is the number of multipaths per user, K is the number of active users in the system, and $d(x, c_i)$ is the non-negative distortion measure.

We will make reference to these important variables during the following sections. However, we should note at this point that the system we are evaluating has only one user and is an isolated wireless system making variables K and M_c equal to one.

4.1 .tif to .jpg

As the first step in both simulations, we must take a .tif image and compress it using a basic JPEG compression algorithm. To achieve this we utilize the Discrete Cosine Transform reviewed above and implement it in Matlab as follows.

First, we define an 8×8 transform matrix using the 'dctmtx(8)' command, where the 8 specifies the dimension of the matrix. This command outputs the following

$$T_{pq} = \begin{cases} \frac{1}{\sqrt{M}}, & \text{if } p = 0 \leq q \leq M - 1. \\ \sqrt{\frac{2}{M}} \cos \frac{\pi(2q+1)p}{2M}, & \text{if } 1 \leq p \leq M - 1 ; 0 \leq q \leq M - 1. \end{cases} \quad (4.3)$$

Once this has been accomplished we apply the two dimensional (2D) DCT to individual 8×8 blocks using the following operation

$$jpg_{in} = [\mathbf{T}][\mathbf{Im}][\mathbf{T}'] \quad (4.4)$$

where Im are the 8×8 image blocks obtained from the TIF figure, T is the DCT matrix and T' is the DCT matrix transpose.

Finally we multiply the 8×8 blocks by a mask to eliminate some of the frequency components of the image, as previously described. The mask that we choose to apply, in order to eliminate the high frequency coefficients, is the following

1	1	1	1	0	0	0	0
1	1	1	0	0	0	0	0
1	1	0	0	0	0	0	0
1	0	0	0	0	0	0	0
0	0	0	0	0	0	0	0
0	0	0	0	0	0	0	0
0	0	0	0	0	0	0	0
0	0	0	0	0	0	0	0

The resulting coefficients are the JPEG quantized coefficients that will be used.

4.2 Quantization

4.2.1 Variable Uniform Quantization

As reviewed above, variable uniform quantization refers to two different aspects of the quantization process. The uniform aspect is achieved very simply by quantizing each coefficient obtained by the above procedure.

Variable quantization on the other hand can be achieved in various ways. In this thesis, we chose to adopt Lloyds Matlab algorithm in order to obtain the variable step sizes needed for this quantization. Furthermore, taking advantage of the flexibility of JPEG to meet our needs and restrictions we chose to use a 9 bit coefficient alphabet for the compression scheme.

More specifically, we were able to apply Lloyds variable step size quantization algorithm using the `lloyds(training_set, initcodebook)` matlab command. This command optimizes the scalar quantization output parameters, partition and codebook, for the provided training data in the vector `training_set`. The initial guess of the codebook values is given by `initcodebook`. The output codebook is a vector of the same length as `initcodebook` and its partitions are defined by a vector whose length is one less than the length of the codebook. The algorithm uses an iterative process to try to minimize the mean square distortion error. The optimization processing ends when either:

- Relative change in distortion between iterations is less than 10^{-7}
- The distortion is less than $eps * max(training_set)$, where `eps` is MATLAB's floating-point relative accuracy

4.2.2 Channel Optimized Vector Quantization

On the other hand, performing a channel optimized vector quantization is a bit more complex. The channel optimized vector quantization technique used in this thesis is depicted in figure

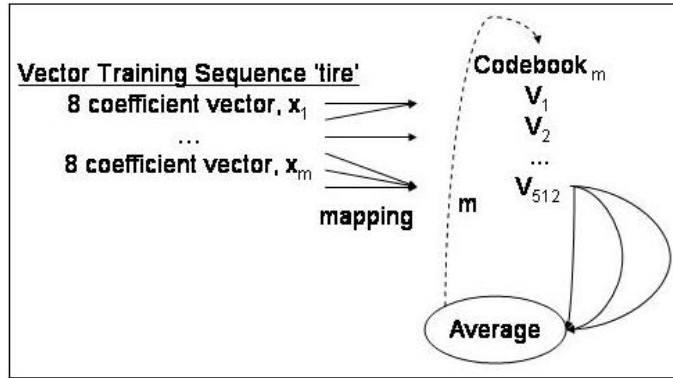


Figure 4.1: Vector Quantization

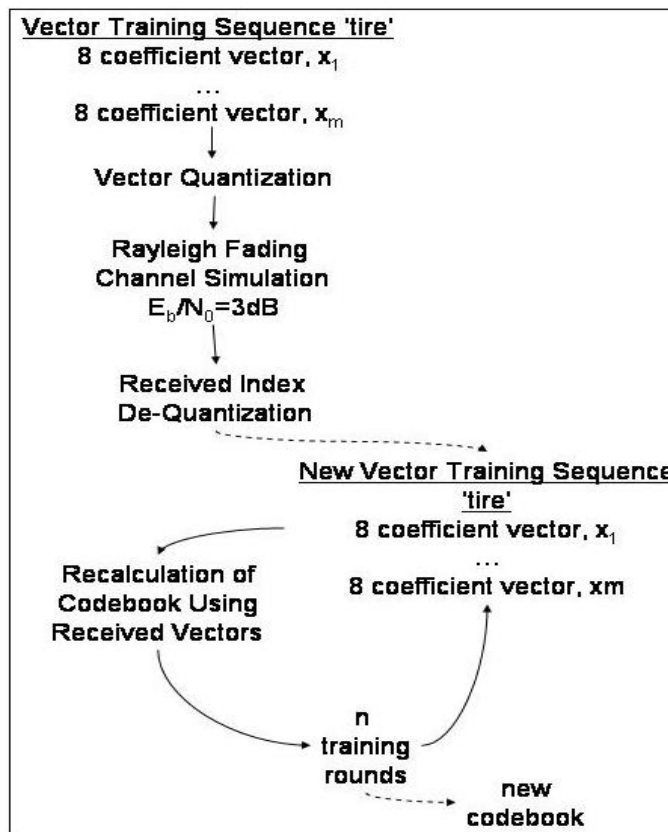


Figure 4.2: Channel Optimized Vector Quantization

[4.2]. As reference, it is also important to remember the basic idea behind vector quantization depicted here:

In order to perform a COVQ and obtain the trained codevectors we need to follow the

next steps:

1. The picture whose vectors are going to be used to construct the codebook is transformed by means of the same procedure explained above, from .tif to .jpg.
2. Vector Quantization is performed on this data in order to obtain a transmission codebook. Specifically, we use the LVQ1 algorithm from the SOM toolbox to train the codebook vectors. In the algorithm, Codebook contains a fixed number of vectors S_i and so does the data vector X_j . Both vector sets are classified where classes are set to the first column of data or map structures. For each X_j there is defined the nearest codebook vector index c by searching the minimum of the euclidean distances between the current X_j and codebook vectors S_i

$$c = \min \{ \|X_j - S_i\| \}, \quad i = [1, \dots, 512], \text{ and fixed } j. \quad (4.5)$$

The LVQ1 algorithm trains the codebook vectors for a set number of times defined by the parameter r_{len} in the function. S_c is updated as follows for each training sequence

$$S_c(\text{updated}) = \begin{cases} S_c(\text{old}) + \alpha * (X_j - S_c(\text{old})), & \text{If } X_j \text{ and } S_c \text{ belong to the same class.} \\ S_c(\text{old}) - \alpha * (X_j - S_c(\text{old})), & \text{If } X_j \text{ and } S_c \text{ belong to different classes.} \\ \text{Otherwise} & \text{No updating.} \end{cases} \quad (4.6)$$

3. Once a VQ codebook is obtained the same data is sent through the Rayleigh fading channel using distinct values of E_b/N_0 , they are then decoded.
4. The new data is then used as the new vector training sequence X_j and it is used to repeat the VQ process which now gives us the channel optimized vector quantization codebook.

The result of this process is a locally optimum encoding rule for mapping source vectors to fixed length binary indices and a corresponding decoding rule for mapping binary indices to their associated codewords, which may or may not be unique. In other words, the decision region which defines each codebook vector is now trained for this specific channel.

Hence the iterative process presented here optimizes the encoding areas that are assigned to each of the c_i codewords that represent an eight coefficient vector. This optimization, accomplished after 512 iterations of the learning vector process aims at minimizing the cost function presented previously by creating the optimum encoding region for each codevector.

It is also important to remember that the variables $d(x, c_i)$ and $P(c_i)$ from the mathematical expression in equations [4.1] and [4.2], which are the distortion measure and the

probability of transmission of a given index from the codebook (c_i), are implicit in the VQ algorithm and the JPEG image coding process respectively. Never the less, because the JPEG image coding process is extremely variable and has no probability distribution function which characterizes it, the two variables are difficult to model mathematically, and hence results involving JPEG coding are best obtained via a mathematical simulation.

4.3 Decimal to Binary

Once we obtain the 4096 coefficients for the Variable Uniform Quantization and 512 coefficients for the Channel Optimized Vector Quantization we are almost ready to transmit this information. First, however, we employ a simple function to convert each coefficient into its 9 bit binary representation. After conversion, the bits are serialized and are ready to introduce into the transmission simulation.

All together, once coded, Lloyds Uniform Variable Quantization utilizes a total of 36864 bits to represent the information, while the VQ algorithm only needs 4608 bits to represent the same image. In general, our VQ algorithm has achieved a better quantization and will therefore need to transmit less information over our Rayleigh fading channel.

4.4 Transmission of data

Once information has been serialized and is prepared for transmission, we jump into the next phase of the simulation which is the transmission of data. We have subdivided this part into several subsections which are reviewed next.

4.4.1 The QPSK modulation

In order to implement the QPSK modulation we call the function *qpskmod* from the main program. The function takes the information vector input into the simulation, and splits the information in two, one vector for each modulation level. The division of information is performed on pair of bits rather than on the entire vector using the following mathematical equations implemented in a loop

$$isi = isi + 2^{(m2-ii)} \times paradata2((1 : para), ii + count2); \quad (4.7)$$

$$isq = isq + 2^{(m2-ii)} \times paradata2((1 : para), m2 + ii + count2); \quad (4.8)$$

which in general takes a binary input vector such as

1 -1 -1 -1 -1 -1 1 1 -1 -1 -1 1 1 -1 1 1

and outputs two sequences as follows

$$\begin{matrix} 1 & -1 & -1 & 1 & -1 & -1 & 1 & 1 \\ -1 & -1 & -1 & 1 & -1 & 1 & -1 & 1 \end{matrix}$$

The output of this function are the in-phase channel (i-channel) and quadrature-phase channel (q-channel). The two vectors are then fed into the spreading function *spread* reviewed in the next sub-section to implement the CDMA access technique.

4.4.2 The CDMA access technique

By using the functions *mseq* and *goldseq* defined by the CDMA simulation programmed by H.Harada and T.Yamamura, we are able to create the CDMA gold sequence that will be used to perform the spreading on our data.

The *mseq* function generates an M-sequence or Shift-Register sequence for an n register system. The sequences produced are not orthogonal, but they do have a narrow autocorrelation peak. The name already makes clear that the codes can be created using a shift-register with feedback-taps. In this simulation we use the following set of equations implemented in a for loop to determine the individual M-sequences, as seen in the following figure

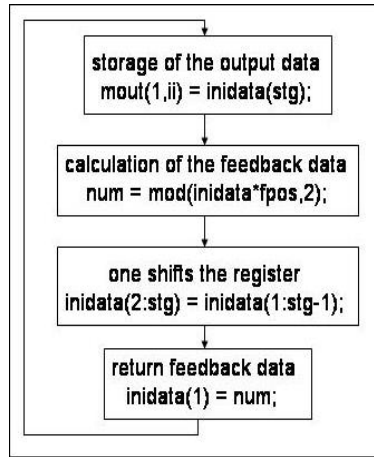


Figure 4.3: M-Sequence Construction

Note that the number of possible codes is dependent on the number of possible sets of feedback-taps that produce each M-sequence.

By combining two distinct M-sequences we are able to obtain a Gold code. In the simulation we utilize the function *goldseq*, to which we input two distinct M-sequences, to obtain the Gold code. The implementation of the Gold sequence is done by means of the following equation

$$(Msequence_1) \otimes (Msequence_2) \tag{4.9}$$

Once we have obtained our gold sequence which we call *code*, we use the function *spread* to apply the spreading on the i-channel and q-channel of our QPSK modulated data obtained as described in the previous section.

The spreading function that is applied to our i-channel and q-channel is based on the following set of equations

$$iout = reshape(rot90(gold - code) * idata, 1, size) \quad (4.10)$$

$$qout = reshape(rot90(gold - code) * qdata, 1, size) \quad (4.11)$$

where we multiply a ninety degree rotated version of our gold sequence obtained above by either our *idata* or *qdata* vector. This process accomplishes the spreading of our signal. Once we have our spread signal, we reshape the matrix into a single one dimensional vector in order to prepare it for transmission.

Now that we have our QPSK modulated CDMA spread signal, we are nearly ready to transmit our information. Prior to transmission we pass our i-channel and q-channel vectors through a Nyquist filter defined by the matlab function *hrollfcoef* which is an odd length linear phase Finite Impulse Response Filter.

These filters have the unique property that every k^{th} impulse response sample is zero except for the central coefficient. The placement of the zero samples in the filter matches locations of the non-zero samples in the upsampled signal which allows these samples to remain unchanged as a result of the interpolation operation. The ideal Nyquist filter of order k has a frequency response with a cut off at $\frac{1}{2k}$ Hz.

In particular, the implementation of our filter given by the function *hrollfoef* gives us the response in figure [4.4]

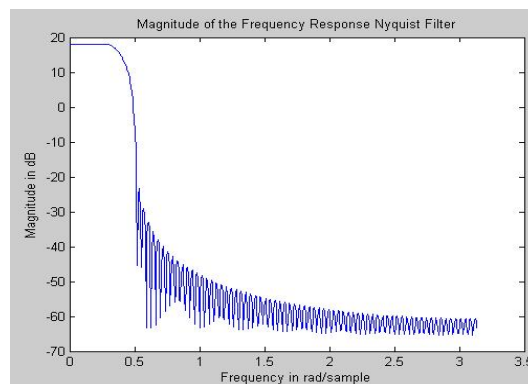


Figure 4.4: Frequency Response Nyquist Filter

The filter is implemented convolutionally within the main program by means of the following equation

$$y(n) = \sum_{m=-\infty}^{\infty} x(m)h(n-m) \quad (4.12)$$

where the function performs the convolution between signal and filter. Hence the above algorithm passes the *idata* and *qdata* information convolutionally through the Nyquist filter.

4.4.3 The transmission of the encoded image through a wireless Rayleigh fading channel

In order to implement the Rayleigh fading channel, we must first review the choice of attenuation levels for the reflected waves which we have used in this simulation. Specifically, we have decided to use an obstructed sight (OBS) model, in which we basically imagine ourselves in an office building. The attenuation levels which we have chosen for each of the 6 multipath waves, *L*, which the receiver is going to pick up are the following

$$[10.0,16.0,16.0,27.0,30.0,35.0] \text{ (dB)}$$

and are expressed in decibels. Furthermore, they arrive with the following delay times with respect to the transmission time (the delays are given with respect to the time resolution of the simulation, given in part by the symbol transmission rate specified at 256×10^3 Bps)

$$[2,3,4,5,8,10] \text{ (s)}$$

Lastly, we must also input the vector that defines the initialized phase for each of the multipath waves which we have chosen as follows

$$[0.3,5.9,10.0,25.0,50.0,90.0] \text{ (degrees)}$$

In order to implement the Rayleigh fading the main program calls the function *sefade*. The function calls two other important functions, one which implements the fading itself, *fade* and the other which delay's the multipath waves, *delay* which will also be explained.

If we explore the function *sefade* we notice that this function mathematically manipulates the information obtained from the attenuation and initial phase delay vectors reviewed above. Specifically, *sefade* changes the attenuation levels from decibel into decimal notation, and changes our initial phase delay vector from degree into radian notation by means of the following equations

$$atts = 10^{(-0.05 \times dlvl(k))} \quad (4.13)$$

$$theta = th(k) \times pi/180.0 \quad (4.14)$$

It also defines a total attenuation factor

$$total_attn = sum(10^{(-1.0 \times dlvl/10.0)}) \quad (4.15)$$

which is later applied on the output vector that has passed through the other two functions, *delay* and *fade*.

Once we have this information, we are ready to first implement the delay of the signal by means of the function *delay*. Inside this function we find a matrix manipulation of the i-phase and q-phase vectors. Specifically, vector samples are delayed for each of the multipath waves according to the delay times specified previously by means of the following for either the i-channel or q-channel

$$out(idel + 1 : nsamp) = idata(1 : nsamp - idel); \quad (4.16)$$

where *idel* are the delay times specified in the vector above for each multipath wave.

The most important function within the simulation is possibly the fading function within *sefade*. Note that this function, *fade*, determines the variance σ^2 of the Rayleigh fading process. If we review the simulation, we can see that we define two basic constants, *xc* and *xs* based on the number of samples, doppler frequency, and normalized power given by

$$power\ normalized\ factor = \sqrt{\frac{1.0}{(2.0 \times (fading\ waves))}} \quad (4.17)$$

The main difference between the two constants, *xc* and *xs*, is that one is multiplied by the power normalized i-channel and the other by the power normalized q-channel. By taking the sum of the squares of these two parameters

$$\sqrt{xc^2 + xs^2} \quad (4.18)$$

and multiplying it by our i-data and q-data we obtain our output spread signals for our i-channel and q-channel respectively.

Finally the last part of the transmission simulation is to add white Gaussian noise to the i-channel and q-channel using the function *comb2*. The function calculates an attenuation value based mainly on the E_b/N_0 value which is specified, other factors such as the symbol rate are also taken into consideration. This attenuation factor, which has the characteristics of white gaussian noise, is then added to our i-channel and q-channel data to complete the transmission simulation.

4.5 Receiver

The receiver first passes the information through the Nyquist convolutional filter explained in one of the preceding sections. Once this has been achieved, and after some manipulation we proceed to first de-spread the signal using the *despread* function which basically performs the inverse spreading of the signal explained previously. Notice that the gold code obtained

for the transmitter must be shared by the receiver in order to accurately de-spread the received signal.

Finally we de-modulate the qpsk signal using the *qpskdemod* function which once again simply performs the inverse process used to modulate the information in the transmitter.

4.6 Binary to decimal

Once the information vector has been received in binary form, we must convert the vector back to its original coefficients. To do this, we simply re-organize the binary coefficients into 9 bit vectors and convert each vector into its decimal representation. The resulting operation leaves us with the quantization coefficients.

4.7 De-Quantization of received coefficients

The de-quantization of the coefficients is very similar in both cases. In general, once the coefficients are received, the simulation looks up each coefficient in the codebook, which should be shared by both the transmitter and receiver at all times. By looking for each parameter, the quantized value can be extracted and hence the image recovered.

Notice that this technique applies to both the quantization techniques. The codebook is hence a standard codebook in both cases which means that both the transmitter and receiver must have the information to appropriately de-quantize the information.

4.8 JPEG decoding

JPEG decoding is simpler than JPEG coding since the mask that was utilized to eliminate frequency coefficients is no longer used. Hence JPEG decoding is simply a matter of organizing the recovered coefficients and applying the inverse 2D discrete cosine transform by using the following equation

$$tif_{out} = [\mathbf{T}'][\mathbf{Im}][\mathbf{T}] \quad (4.19)$$

where T is the DCT matrix and T' is its transpose. Im is the information that is dequantized and received after being sent through the simulation. Notice that the inverse 2D DCT is performed by changing the order of matrix multiplication.

The result of this transformation is the received image that has been transmitted through the Rayleigh fading simulation.

5 Results

In this section we present the results obtained from our simulation. First we will review the original images used to execute the simulation. Later we will present the two original images in their compressed format. Then, we will review images of our variable uniform quantization algorithm, as well as our COVQ algorithm that have been transmitted and affected by our Rayleigh fading model simulation. In our last section we will review two graphs comparing the performance of both algorithms.

5.1 Original Images

Before presenting the images that show the results that we obtained from the simulations we will first display the original images that are used in this simulation (because of memory and time limitations when transmitting the image it was reduced to an appropriate size presented in the second figure).



Figure 5.1: Original Complete Picture Used in Transmission

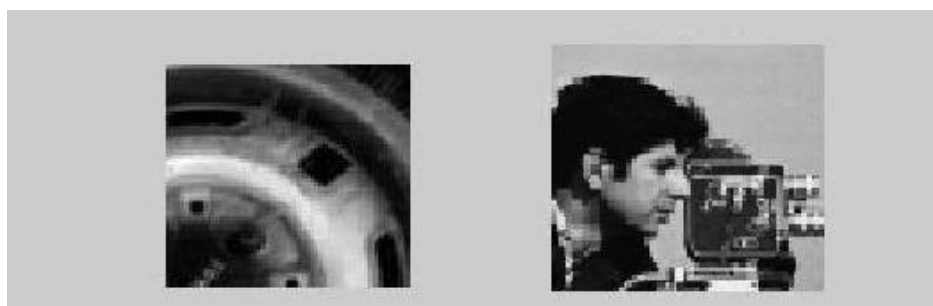


Figure 5.2: Original Fraction of Picture

5.2 Original Quantized Images

In this subsection we will display the images that are obtained once they are quantized using the presented algorithms without passing the images through the Rayleigh fading channel.

In the following figures, the first image is once again, the original image without scaling, the second image is the quantized image without scaling and the third image is a blown up image of the second image to show the details of the picture. Remember, both quantization techniques used a nine bit coding scheme per symbol to be transmitted.

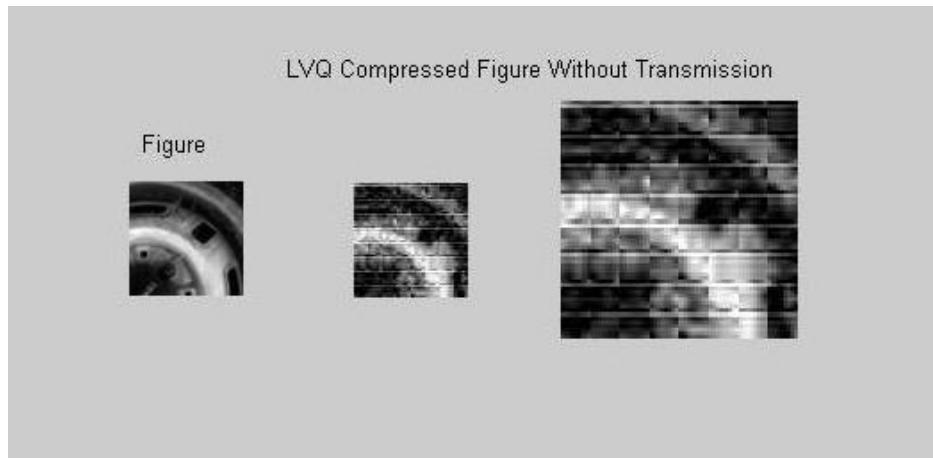


Figure 5.3: LVQ Quantization Without Transmission of tire.tif

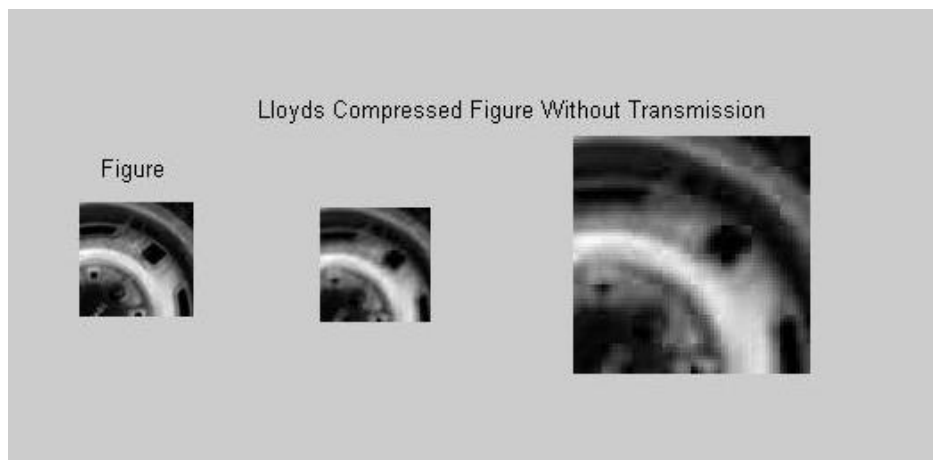


Figure 5.4: Lloyds Quantization Without Transmission of tire.tif

In the images it is important to note that the visible overall neatness of the figure compressed with Lloyds Variable Uniform Quantization is better than that of the LVQ Quantized

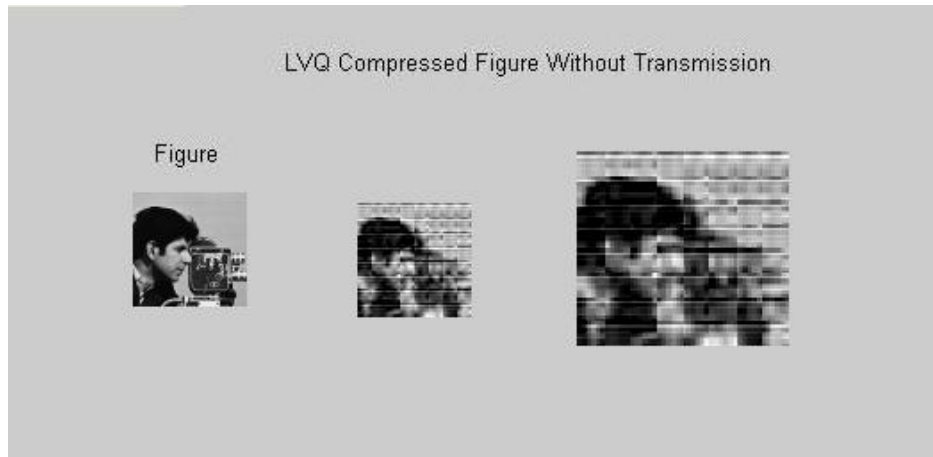


Figure 5.5: LVQ Quantization Without Transmission of Cameraman.tif

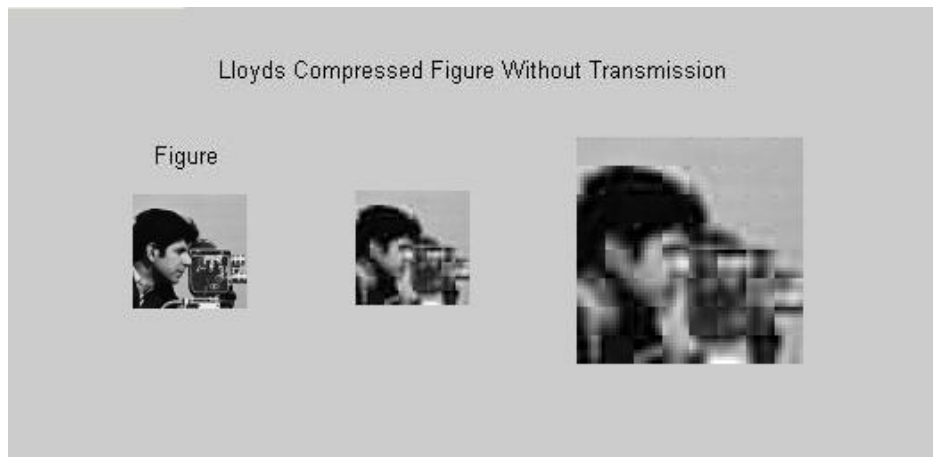


Figure 5.6: Lloyds Quantization Without Transmission of Cameraman.tif

image. After several measurements, we determined that the average MSE, in comparison to the original image, was about 0.0600 for Lloyds algorithm, and 0.0900 for the LVQ algorithm. The MSE of the LVQ algorithm can be explained because of the 512 coefficient codebook that is used to quantize the image and whose coefficients can be represented by 9 binary bits. In general, compression of these images by means of Lloyds algorithm utilizes a total of $64 \times 64 \times 9 = 36864$ bits, where in comparison, LVQ compression needs a total of $512 \times 9 = 4608$ bits to represent the image; hence the difference in quality at this point.

5.3 Received Pictures

Now that we have seen the image that is going to be transmitted, we will finally review a series of pictures obtained from the simulation that was explained above. The explanation of the parameters used for each of the results can be seen in the image header and will be restated in the last subsection of this section. However, a general understanding of what the picture represents can be obtained from the captions that accompany each picture.

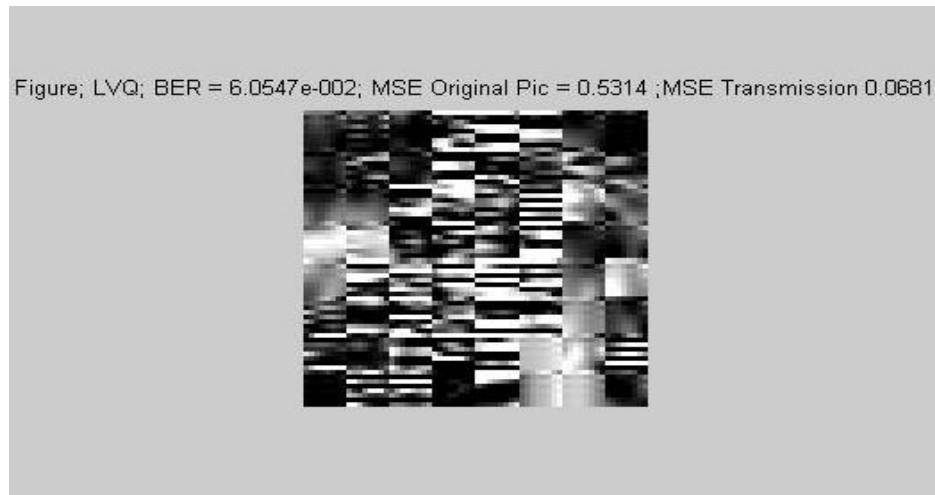


Figure 5.7: $E_B/N_0=1$ dB Using LVQ Quantization



Figure 5.8: $E_B/N_0=1$ dB Using Lloyds Quantization

Figure; LVQ; BER = 4.839e-002; MSE Original Pic = 0.4889 ;MSE Transmission 0.0544



Figure 5.9: $E_b/N_0=2$ dB Using LVQ Quantization

Figure; Lloyds; BER = 2.5987e-002; MSE Original Pic = 0.8061 ;MSE Transmission 0.2339



Figure 5.10: $E_b/N_0=2$ dB Using Lloyds Quantization

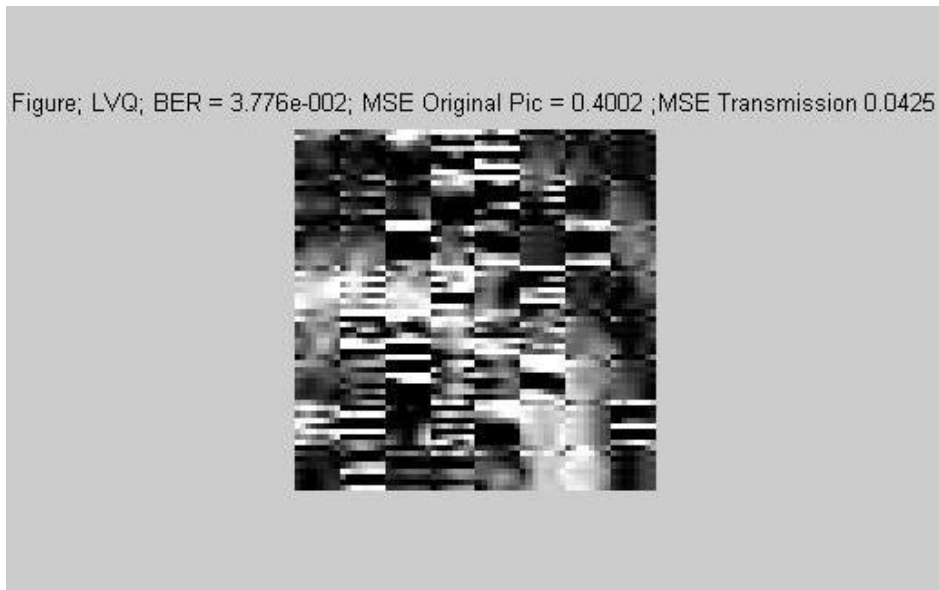


Figure 5.11: $E_B/N_0=3$ dB Using LVQ Quantization



Figure 5.12: $E_B/N_0=3$ dB Using Lloyds Quantization

Figure; LVQ; BER = 2.8211e-002; MSE Original Pic = 0.3249 ;MSE Transmission 0.0317

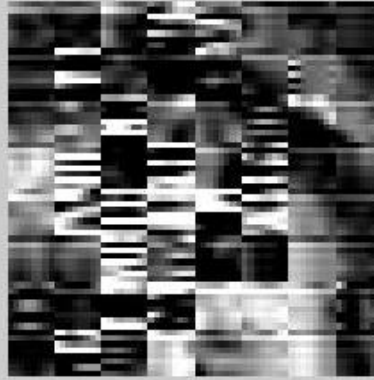


Figure 5.13: $E_B/N_0=4$ dB Using LVQ Quantization

Figure; Lloyds; BER = 1.166e-002; MSE Original Pic = 0.4251 ;MSE Transmission 0.1050



Figure 5.14: $E_B/N_0=4$ dB Using Lloyds Quantization

Figure; LVQ; BER = 2.191e-002; MSE Original Pic = 0.2581 ;MSE Transmission 0.0247



Figure 5.15: $E_B/N_0=5$ dB Using LVQ Quantization

Figure; Lloyds; BER = 8.382e-003; MSE Original Pic = 0.3192 ;MSE Transmission 0.0754



Figure 5.16: $E_B/N_0=5$ dB Using Lloyds Quantization

Figure; LVQ; BER = 1.584e-002; MSE Original Pic = 0.2012 ;MSE Transmission 0.0178



Figure 5.17: $E_B/N_0=6$ dB Using LVQ Quantization

Figure; Lloyds; BER = 5.262e-003; MSE Original Pic = 0.2158 ;MSE Transmission 0.0474



Figure 5.18: $E_B/N_0=6$ dB Using Lloyds Quantization

5.4 Generalized Results

In this subsection we will review the overall results. The two graphs, [5.19][5.20], display the information that is summarized in the table that follows them. By means of the table or graphs we can compare the results obtained after applying the algorithms reviewed throughout this paper and more importantly, prove that by using a COVQ algorithm we are effectively able to reduce the amount of errors introduced by this specific transmission medium, an 800MHz Rayleigh fading channel, into our image.

From the graphs and information in the table we can observe that our COVQ algorithm is effective at improving the transmission of digital JPEG images over a Rayleigh fading channel. In general, we can clearly see that for values of E_b/N_0 which are small, which implies a noisier channel, our COVQ outperforms the variable uniform quantization significantly. However, as our E_b/N_0 increases, and the channel becomes more ideal, our COVQ and variable uniform quantization performance become almost identical. Never the less, given that our compression using our COVQ is 8 times more efficient, it would still be wise to consider a COVQ or VQ algorithm instead of our variable uniform quantization in nearly ideal conditions.

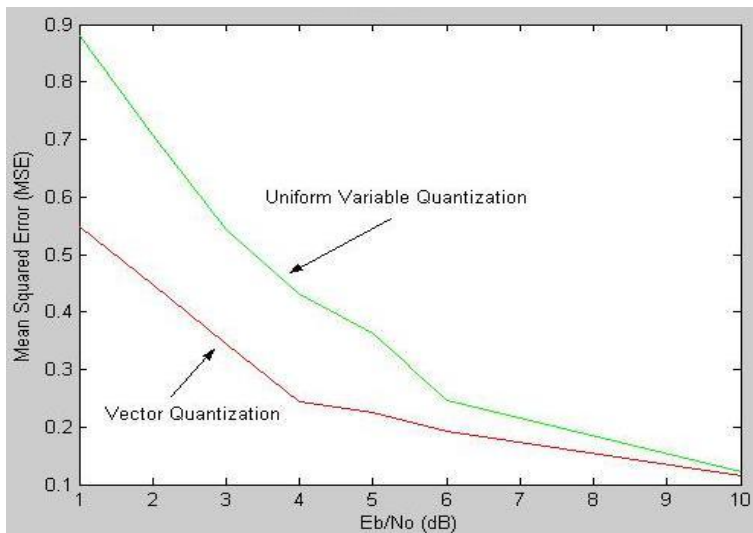


Figure 5.19: Resulting MSE using Lloyds vs. LVQ Quantization of tire.tif

Another important result that must be mentioned is that the COVQ algorithm helps to find a locally optimum encoding rule for mapping source vectors to fixed length binary indexes given specific channel conditions. Hence the iterative process used to find the encoding regions, which is repeated 512 times, minimizes the cost function presented earlier by

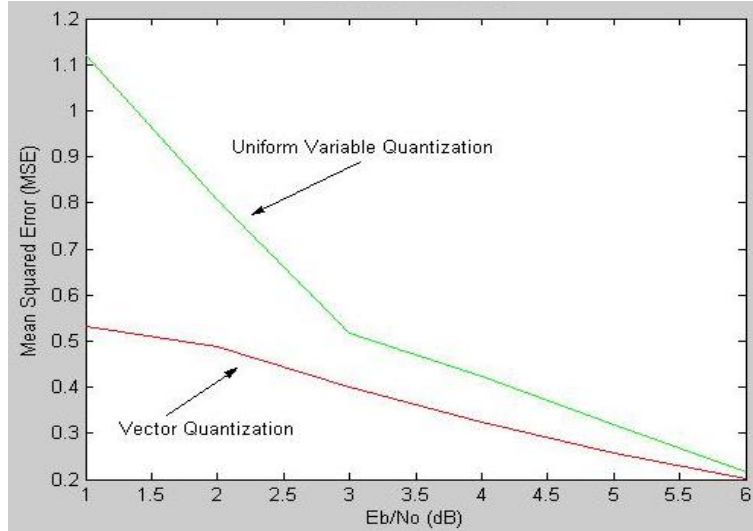


Figure 5.20: Resulting MSE using Lloyds vs. LVQ Quantization of cameraman.tif

Quantization	E_b/N_0	Tire.tif MSE	Cameraman.tif MSE
COVQ	1	0.5314	0.5480
Lloyds	1	1.1187	0.8790
COVQ	2	0.4889	0.4480
Lloyds	2	0.8061	0.7064
COVQ	3	0.4002	0.4002
Lloyds	3	0.5163	0.3448
COVQ	4	0.3249	0.5428
Lloyds	4	0.4251	0.2430
COVQ	5	0.2581	0.4311
Lloyds	5	0.3192	0.3192
COVQ	6	0.2012	0.1922
Lloyds	6	0.2158	0.2468

Table 5.1: Results for tire.tif and cameraman.tif

optimizing the vector coding for the specific channel. More specifically, by finding the optimum encoding regions, the parameter $P(c_i)$, which represents the probability of associating a codeword with its corresponding vector, is maximized for the specific channel condition by means of a COVQ.

6 Conclusions

As mentioned previously, JPEG is a block based video coding scheme that achieves compression by removing spatial and temporal redundancy. In order to achieve this each picture is divided into 8×8 blocks which are encoded using the 2 dimensional discrete cosine transform. After the DCT has been applied to each block they are quantized using variable uniform quantization to reduce the number of coefficients which are then coded and prepared for transmission over the channel.

In this thesis we demonstrate that by adopting a joint source channel code design and using information from the channel to construct our quantization scheme we can transmit JPEG images over a Rayleigh Fading Channel more successfully.

In order to prove our hypothesis we use a model to simulate the effects of a Rayleigh fading channel on our JPEG compressed image. In general, it is important to remember that the Rayleigh fading channel is characterized by two important parameters that inhibit our ability to accurately transmit information the attenuation factor and the additive white Gaussian noise.

Once we had constructed, tested and compared our results, we arrived at the following important conclusions:

- By using a channel optimized vector quantization we are able to significantly reduce the effects of the Rayleigh fading channel on our transmitted message.
- Our channel optimized vector quantization not only improved the transmission of our information over the Rayleigh fading channel, it also achieved a compression 8 times more efficient than with the normal variable uniform quantization.
 - Because we have achieved a more efficient compression with a similar quality, we can consider inserting parity bits in the channel coding to increase the robustness of our transmission while still transmitting less bits than with our original compression technique.
 - We can also consider increasing our code vector alphabet, and consider using a 1024, or 2048 vector alphabet with 10 or 11 bit coefficients instead of the 9 bits that we use in this simulation. By using a 2048 vector alphabet, our transmission length in this specific experiment would increase from 4608 bits to 5632, which is still extremely small in comparison to the 36864 bits that are transmitted with the non-optimized quantization technique.
- In general, our COVQ has achieved a better compression, and has effectively helped to reduce the MSE during the transmission of information over our Rayleigh fading channel.

- Note that this COVQ algorithm is designed for the specific channel which we have consider. It is more than likely that such an algorithm would be sub-optimal if an ideal, or other type of environment where considered.

6.1 Future Work

As observed above, our COVQ has achieved a significant reduction in size in comparison to our variable uniform quantization. Future work in this specific area could involve finding the optimum vector alphabet size, without surpassing the number of bits used in the original compression algorithm, to optimize transmission of information using this technique.

Additional future work could involve applying the same algorithm that is utilized here to MPEG video. As reviewed earlier, MPEG is very similar to JPEG, with the exception that MPEG must use more sophisticated compression algorithms to avoid redundancy within frames.

A Additional Results

Figure; LVQ; BER = 3.776e-002; MSE Original Pic = 0.5480 ;MSE Transmission 0.0425

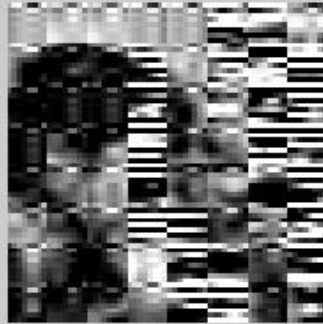


Figure A.1: $E_B/N_0=1$ dB Using LVQ Quantization

Figure; Lloyds; BER = 3.9337e-002; MSE Original Pic = 0.8790 ;MSE Transmission 0.3540



Figure A.2: $E_B/N_0=1$ dB Using Lloyds Quantization



Figure A.3: $E_B/N_0=2$ dB Using LVQ Quantization



Figure A.4: $E_B/N_0=2$ dB Using Lloyds Quantization



Figure A.5: $E_B/N_0=3$ dB Using LVQ Quantization



Figure A.6: $E_B/N_0=3$ dB Using Lloyds Quantization

Figure; LVQ; BER = 1.649e-002; MSE Original Pic = 0.2430 ;MSE Transmission 0.0186

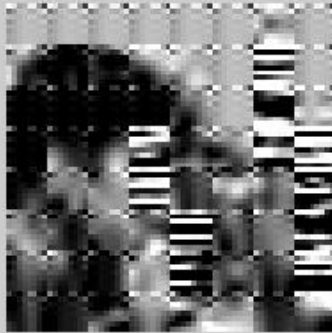


Figure A.7: $E_B/N_0=4$ dB Using LVQ Quantization

Figure; Lloyd; BER = 1.6086e-002 MSE Original Pic = 0.4311 ;MSE Transmission 0.1448



Figure A.8: $E_B/N_0=4$ dB Using Lloyds Quantization

Figure; LVQ; BER = 7.5954e-003; MSE Original Pic = 0.2252 ;MSE Transmission 0.0085

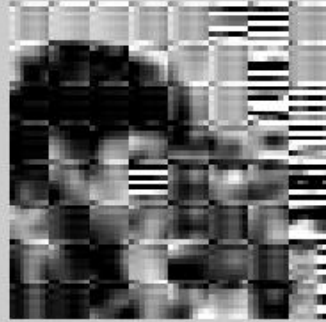


Figure A.9: $E_B/N_0=5$ dB Using LVQ Quantization

Figure; Lloyd; BER = 1.258e-002 MSE Original Pic = 0.3631 ;MSE Transmission 0.1133



Figure A.10: $E_B/N_0=5$ dB Using Lloyds Quantization

Figure; LVQ; BER = 8.897e-003; MSE Original Pic = 0.1922 ;MSE Transmission 0.0100



Figure A.11: $E_B/N_0=6$ dB Using LVQ Quantization

Figure; Lloyd; BER = 7.676e-002 MSE Original Pic = 0.2468 ;MSE Transmission 0.0691



Figure A.12: $E_B/N_0=6$ dB Using Lloyds Quantization

Figure; LVQ; BER = 1.085e-003; MSE Original Pic = 0.1161 ;MSE Transmission 0.0012

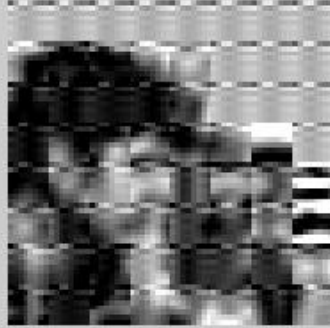


Figure A.13: $E_B/N_0=10$ dB Using LVQ Quantization

Figure; Lloyd; BER = 2.577e-003 MSE Original Pic = 0.1212 ;MSE Transmission 0.0232



Figure A.14: $E_B/N_0=10$ dB Using Lloyds Quantization

References

- [1] Abramson, Norman. *Information Theory and Coding*. New York: McGraw Hill, 1963.
- [2] Arch C. Luther. *Principles of Digital Audio and Video*. Boston: Artech House Publishers, 1997.
- [3] Bernhardt, R.C. “*Macroscopic diversity in frequency reuse systems.*” IEEE Journal on Selected Areas in Communications, No. 5, June 1987, pp. 862-870.
- [4] Breed, Gary. “*Signal Propagation in the 900 MHz to 5 GHz Wireless Bands*”. High Frequency Electronics, No. 9, September 2003 pp. 59-60.
- [5] Chen, Tsuhan. *Special Topics in Signal Processing. Multimedia Communications: Coding, Systems and Networking*. Pittsburgh: Lectures CMU.EDU, 1999.
- [6] Cordoba, Dr. Jose Luis R. *Estudio Sobre La Codificacion Conjunta Canal Fuente en Canales Continuos*. Granada: Universidad de Granada, Nov 2000.
- [7] D.C. Cox, Murray, R. Norris, A. “*800 MHz attenuation measured in and around suburban houses*”. IEEE Journal on Selected Areas of Communications, No. 5, May 1984, pp.198;
- [8] Farvardin, Nariman. “*A study of Vector Quantization for Noisy Channels*”. IEEE Transactions on Information Theory, No. 36, July 1990, pp. 799-809.
- [9] Farvardin, Nariman. “*Design of Channel Optimized Vector Quantizers in the Presence of Channel Mismatch*”. IEEE Transaction on Communications, No. 1, January 2000, pp. 118-124.
- [10] Farvardin, Nariman. “*Joint Design of Block Source Codecs and Modulation Signal Sets*”. IEEE Transaction on Communications, No. 12, December 2001, pp.304-315.
- [11] Farvardin, Nariman, and Vaishampayan, V. “*On the Performance and Complexity of Channel Optimized Vector Quantizers*”. IEEE Transaction Information Theory, No.1, January 1991, pp. 155-160.
- [12] Liu, F.H. and Cuperman, V. “*Joint Source and Channel Coding Using a Non Linear Receiver*”. Proc. IEEE Globecom, 1993 conference.
- [13] Hoenig. McLaughlin Roman K. KTA. Harte, Lawrence. Morris. *CDMA IS-95 for Cellular and PCS*. New York: McGraw-Hill, 1999.
- [14] H. Hashemi. “*The Indoor Radio Propagation Channel*”. Proceedings of the IEEE, No. 81, July 1993, pp. 943-968.

- [15] H. Kumazawa, M. Kasahara, and T. Namekawa “A construction of Vector Quantizers for Noisy Channels”. Electronics Engineering Jpn, No. 67-B, April 1984, pp. 39-47.
- [16] International Telecommunication Union. *Information Technology - Generic Coding of Moving Pictures and Associated Audio Information: Video*. ITU-T Recommendation H.262, 1995.
- [17] Lai, Jersey. Giridhar, Mandyam. *Third-Generation CDMA systems for Enhanced Data Services*. Amsterdam: Academic Press, 2002.
- [18] Lee, Steve. *Spread Spectrum CDMA IS-95 and IS-2000 for RF Communications*. New York: McGraw Hill, 2002.
- [19] Linde, Y. Buzo, A. and Gray, R.M. “An Algorithm for Vector Quantizer Design”. IEEE Transaction Communications, vol. com-28, 1980, pp. 84-95.
- [20] Meikle, Hamish. *Modern Radar Systems*. Boston: Artech House, Boston, 2001.
- [21] Miranda Guardiola, Rolando. *CDMA Soft Handoff Networking Model*. Monterrey Mexico: Masters thesis ITESM Monterrey, December 1997.
- [22] Molkdar, D. “Review on radio propagation into and within buildings”. Proceedings of the IEEE, No.138, February 1991, pp. 61-73.
- [23] Ngan, N. King, Yap, w. Chi, Tan, T. Keng. *Video Coding for Wireless Communication Systems*. England: Marcel Dekker, 2001.
- [24] Rappaport, Theodore S. Seidel, S.Y. “914MHz Path Loss Prediction Models for Indoor Wireless Communications in Multifloored Buildings”. IEEE Transactions on Antennas and Propagation, No. 40, Feb 1992, pp. 1-11.
- [25] Rappaport, Theodore S. *Wireless communications Principles and Practice*. New York: Prentice Hall Communications, 1996.
- [26] Rappaport, Theodore S. Anderson, J.B. Yoshida, S. “Propagation measurements and models for wireless communications channels”. IEEE Communications Magazine, January 1995, pp. 42-49.
- [27] Samuel C. Yang. *CDMA RF System Engineering*. Boston: Artech House Publishers, 1998.
- [28] Skoglund, Mikael. “A Soft Decoder Vector Quantizer for a Rayleigh Fading Channel Application to Image Transmission”. IEEE ISIT January 1994, Trondheim Norway, pp.401.

- [29] Tachikawa Keiji. *W-CDMA Mobile Communications System*. England: John Wiley & Sons, 2002.
- [30] Watkinson, John. *MPEG-2*. England: Focal Press, 1999.
- [31] Young Man Rhee. *CDMA Cellular Mobile Communications Network Security*. New Jersey: Prentice Hall PTR, 1998.
- [32] Zahir, M. Hussein. *BER Performance of DS-SS-CDMA Systems Over Frequency Selective Multipath Rayleigh Fading Channels*. Australia: RMIT University.
- [33] Anonymous. <http://www.ecs.csus.edu/eee/courses/notes/chapter3.pdf>
- [34] Anonymous. <http://dmr.ath.cx/gfx/dct/>
- [35] Anonymous. <http://www.bretl.com/mpeghtml/quantiz.HTM> =Source
- [36] Anonymous. http://netghost.narod.ru/gff/graphics/book/ch09_06.htm
- [37] Anonymous. <http://www.data-compression.com/vq.html#intro>